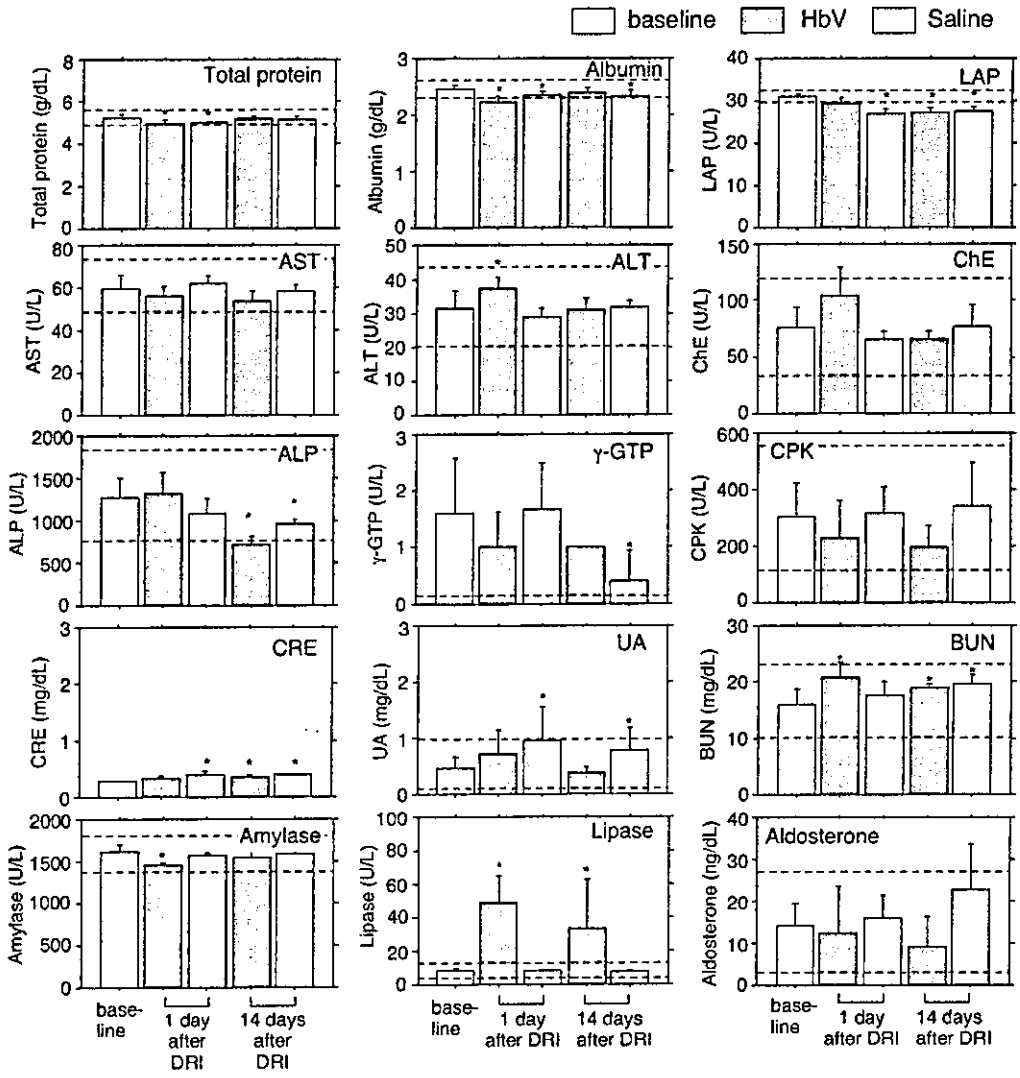

Fig. 6. Plasma clinical chemistry tests reflecting the organ functions such as liver, pancreas, and kidneys and the metabolism of Hb after DRI of HbV or saline. The values are mean ± S.D. *, significantly different versus the baseline group ($p < 0.05$). The dotted lines indicate the levels of 2× S.D. LAP, leucin amino peptidase; AST, aspartate aminotransferase; ALT, alanine aminotransferase; ChE, cholinesterase; ALP, alkaline phosphatase; γ-GTP, γ-glutamyltransferase; CPK, creatine phosphokinase; CRE, creatinine; UA, uric acid; BUN, urea nitrogen.

significant differences between the HbV and the saline groups. Hct and RBC counts decreased significantly for the HbV group, probably due to the dilution of blood by hypervolemia, or suppression of erythropoiesis (release of erythropoietin) because the renal cortex would be exposed to the increased oxygen content in the blood during DRI of HbV as oxygen carriers. The slight hypertension 1 day after DRI would be related to the blood hyperviscosity or hypervolemia due to the presence of HbV. However, the Hct and RBC counts returned to levels similar to those of the saline group 14 days after DRI. The time course of the HbV concentration in plasma indicates that the rate of HbV clearance gradually increased and the concentration reached a plateau, probably due to the nonspecific phagocytic activation of the RES that was clarified previously by a carbon clearance measurement (Sakai et al., 2001). The accelerated liposome clearance of the second infusion was well characterized (Claassen et al., 1988; Laverman et al., 2001); however, its mechanism, antibody formation or complement activation is controversial (Dams et al., 2000; Ishida et al., 2003).

In our previous report, the bolus HbV infusion (20 ml/kg) resulted in significant splenomegaly (about 100% increase) and hepatomegaly (13%) (Sakai et al., 2004b). In the present DRI study, splenomegaly was enhanced (190%), whereas hepatomegaly was similar (14%), indicating that the spleen had a larger capacity for HbV clearance. A large amount of HbV accumulated in the red pulp zone of the spleen and in Kupffer cells of the liver; however, 14 days later it disappeared and the splenohepatomegaly completely subsided. The spleen and the liver showed significant hemosiderin deposition; however, the enzyme concentrations that reflect the liver function did not show any abnormal values.

One day after DRI, the mesangial cells in the renal glomerulus seemed to entrap HbV in their intracellular spaces, and the same portion was stained with Berlin blue 1 and 14 days after DRI. In our previous report on the bolus HbV infusion, there was no abnormality in the kidneys (Sakai et al., 2004b). According to Rudolph et al. (1995), liposome-encapsulated Hb without PEG-modification aggregated in the plasma and showed a slight accumulation in the kidneys. Even though our PEG-modified HbV does not induce intervesicular aggregation, HbV would tend to be aggregated during the longer circulation time due to the DRI. No abnormal value was noted for UA, BUN, and CRE, although urinalysis showed a slight increase in protein levels.

Lipase activity, but not that of amylase, significantly in-

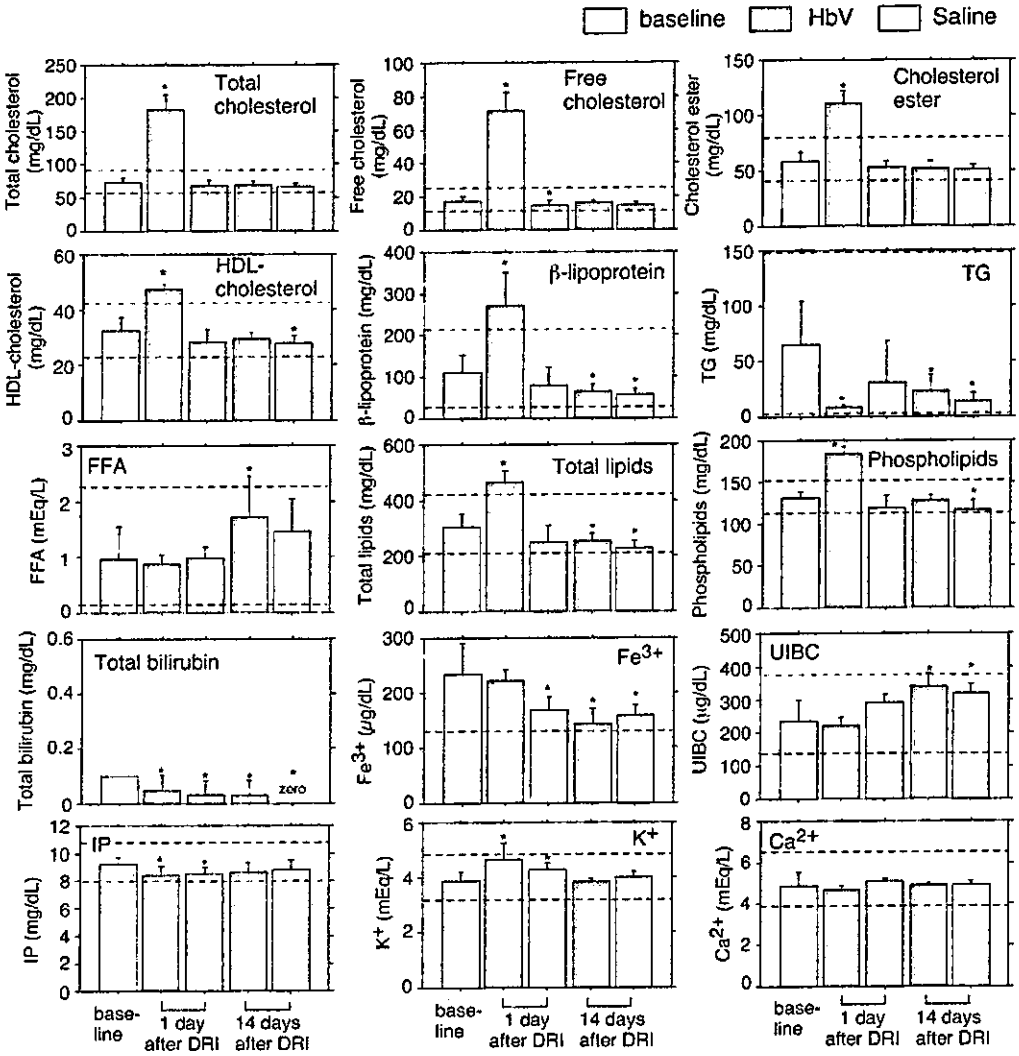

Fig. 7. Plasma clinical chemistry tests reflecting the metabolism of lipids and Hb and electrolytes 1 or 14 days after DRI of HbV or saline. The values are mean ± S.D. *, significantly different versus the baseline group. The dotted lines indicate the levels of 2× S.D. TG, triglyceride; FFA, free fatty acid; UIBC, unsaturated iron-binding capacity; IP, inorganic phosphate.

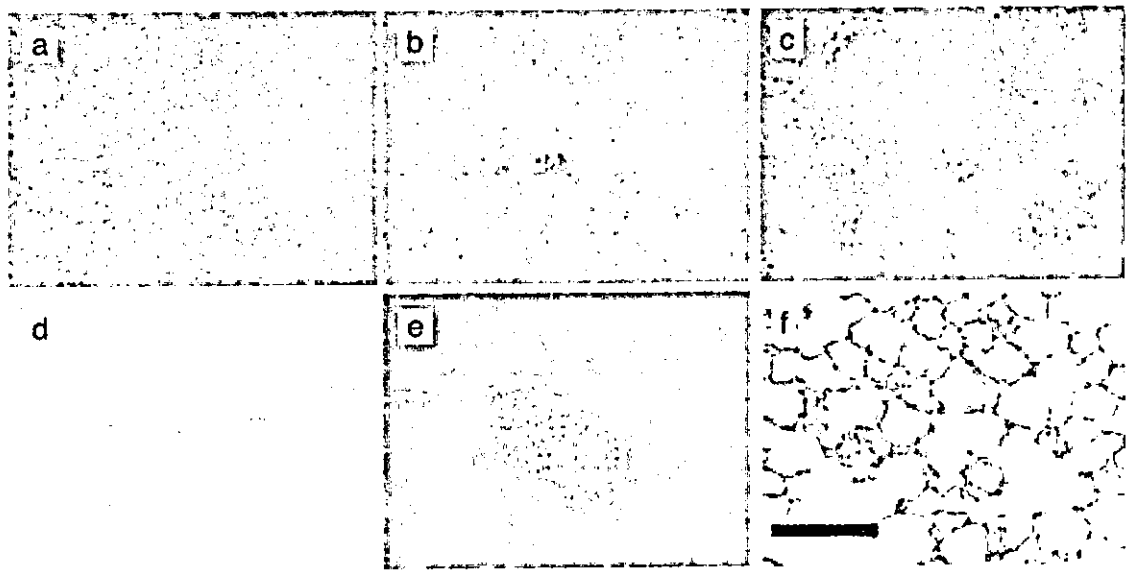

Fig. 8. Histology of spleen (a), liver (b), kidneys (c), heart (d), pancreas (e), and lungs (f) 1 day after DRI of HbV. A significant amount of HbV was accumulated in the red pulp zone of the spleen. The invasion of a significant number of Kupffer cells with HbV was seen in the liver. In the kidneys, the mesangial cells in the renal glomeruli seemed to entrap HbV. The myocardium showed slight staining with Berlin blue. No significant pathological changes are noted in the pancreas and lungs. Scale bar, 100 μm. Hematoxylin and eosin stains (a, b, c, e, and f) and Berlin blue stain (d).

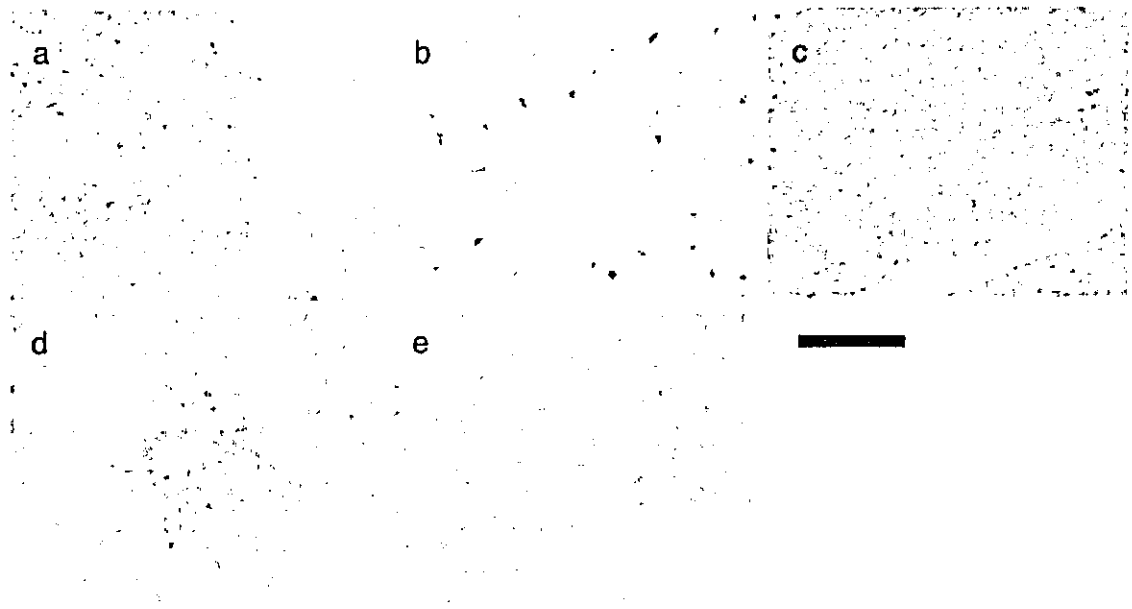

Fig. 9. Histology of spleen (a), liver (b), bone marrow (c), kidneys (d), and adrenal gland (e) 14 days after DRI. Berlin blue staining was performed to examine the presence of hemosiderin. Scale bar, 100 μm.

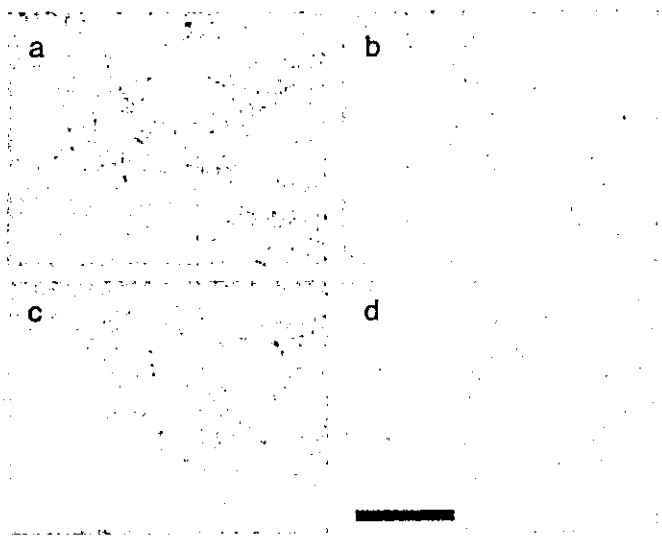

Fig. 10. Double immunohistochemical staining for HO-1 and human Hb in HbV in the rat spleen (a and c) and liver (b and d), 1 (a and b) and 14 days (c and d) after DRI of HbV. The tissues were stained with anti-rat HO-1 monoclonal antibody (GTS-3). The brown-colored portions (a, c, and d) indicate the presence of HO-1, and the pink or gray-beige areas (a and b) indicate the presence of a large amount of HbV. Scale bar, 100 μm.

creased in the HbV group, whereas there was no histopathological abnormality in the pancreas. A similar tendency was observed after the bolus HbV infusion (20 ml/kg) (Sakai et al., 2004b). This level of increment was significantly smaller than the value for the Wistar rats with acute necrotizing pancreatitis that increased the lipase activity from 10 to 475 to 5430 IU/l (Hofbauer et al., 1996). One possible reason for the moderate and specific increase in lipase activity would be related to the enzyme induction in the pancreas by the presence of a large amount of lipids from the liposomes (Stueck-lin-Utsch et al., 2002), because pancreatic lipase hydrolyzes not only triglyceride but also phosphatidylcholine (Rowland and Woodley, 1980). However, the mechanism is not clear, and the pancreatic function should be carefully monitored in the ongoing safety studies.

The plasma lipid components significantly increased after the DRI of HbV. They should be derived from HbV because it contains a large amount of cholesterol and DPPC, and they would be liberated after the HbV particles are captured and degraded in the RES. It is reported that once liposome is captured in the Kupffer cells, the diacylphosphatidylcholine is metabolized and is reused as a cell membrane component or excreted in the bile (Dijkstra et al., 1985; Verkade et al., 1991). Cholesterol is finally catabolized as bile acids in the parenchymal hepatocytes. There should be no direct contact of HbV and the hepatocytes because HbV (diameter, 250 nm) cannot diffuse across the fenestrated endothelium into the space of Disse (Goda et al., 1998). Cholesterol of the vesicles should reappear in the blood mainly as lipoprotein cholesterol after entrapment in the Kupffer cells and should then be excreted in the bile after entrapment of the lipoprotein cholesterol by the hepatocytes (Kuipers et al., 1986). Judging from the results showing that the increases in the plasma lipid components were transient, the lipid components of HbV would gradually be redistributed, metabolized, and excreted in the same manner within 14 days after DRI. However, the details have to be confirmed by the biodistribution of the radiolabeled components.

In spite of the massive HbV infusions, the plasma bilirubin and iron levels did not increase. Urinalysis also showed no increase in the urobilinogen and bilirubin. The anti-human Hb antibody staining detected temporal distributions of HbV in the spleen and liver. The excess amount of heme from Hb in HbV should be metabolized by the inducible form of HO-1 in the spleen macrophages and the liver Kupffer cells, as shown in Fig. 10 (Braggins et al., 1986; Goda et al., 1998). Bilirubin should be excreted in the bile as a normal physiological pathway even during the massive doses of HbV. No increase in the plasma bilirubin level indicated that there was no obstruction or stasis of bile in the biliary tree and that the heme-degrading capacity of the RES did not surpass the ability to eliminate

bilirubin. Berlin blue staining revealed the presence of hemosiderin in the liver, spleen, kidneys, adrenal gland, and bone marrow 14 days after DRI and also in the myocardium 1 day after DRI. Both ferritin and hemosiderein store and release iron molecules, and they are anticipated to induce hydroxyl radical production and succeeding lipid peroxidation. However, iron release from hemosiderin is substantially less than that from ferritin, thus iron molecules in hemosiderin are relatively inert (O'Connell et al., 1989). Multiple blood transfusions often induce hemosiderosis in many organs. Accordingly, Hb encapsulation in the phospholipid vesicles would guarantee the smooth metabolic route of HbV that is similar to the well characterized metabolic route of senescent RBCs in the liver Kupffer cells and spleen macrophages (Bennett and Kay, 1981; Hirano et al., 2001). This would be a great advantage over molecular Hb that incurs not only filtration across the fenestrated endothelium of the glomerular capillary in the kidneys resulting in shorter circulation time and renal failure but also extravasation from the sinusoidal caliber in the liver, causing cancellation of the CO-mediated fail-safe mechanism for conserving sinusoidal patency and bile formation (Kyokane et al., 2001).

In conclusion, all the rats tolerated the DRI of HbV with no deteriorative signs of the organ functions. The phospholipid vesicles for Hb encapsulation would be beneficial for heme detoxification through their preferential delivery to the RES, a physiological compartment for degradation of not only foreign materials but also the senescent RBCs. However, it has to be considered that in humans the circulation time of HbV and its degradation rate in the RES would be different compared with those in rats, because the circulation time of stealth liposomes and the life span of RBCs are different between rodents and humans (Landaw, 1988; Gabizon et al., 2003). A shock condition may also influence on the RES function.

Our results would provide important information not only for the ongoing safety studies of HbV but also for the overall research on liposomal drugs, because this study is the first attempt to infuse repetitively such a large amount of phospholipid vesicles.

Acknowledgments

We acknowledge researchers in the School of Medicine, Keio University; H. Abe, T. Yamaguchi, and S. Kurasaki (Department of Pathology) for excellent histopathological techniques; and Dr. Y. Izumi, Dr. M. Watanabe, and T. Ohba (Department of Surgery) and Dr. M. Kajimura (Department of Biochemistry) for discussions on the experimental procedures.

References

Bennett GD and Kay MM (1981) Homeostatic removal of senescent murine erythrocytes by splenic macrophages. *Exp Hematol* **9**:297–307.

Biro GP and Greenburg AG (1999) Safety toxicology evaluation of *o*-raffinose cross linked hemoglobin solution by daily repeated infusions in rats and dogs (Abstract). *Crit Care Med* **27 (Suppl)**:479.

Braggins PE, Trakshel GM, Kutty RK, and Maines MD (1986) Characterization of two heme oxygenase isoforms in rat spleen: comparison with the hematin-induced and constitutive isoforms of the liver. *Biochem Biophys Res Commun* **141**:528–533.

Chang TM, Lister C, Nishiya, and Varma R (1992) Immunological effects of hemoglobin, encapsulated hemoglobin, polyhemoglobin and conjugated hemoglobin using different immunization schedules. *Biomater Artif Cells Immobil Biotechnol* **20**:611–618.

Charrois GJR and Allen TM (2003) Multiple injection of pegylated liposomal doxorubicin: pharmacokinetics and therapeutic activity. *J Pharmacol Exp Ther* **306**: 1058–1067.

Claassen E, Westerhof Y, Versluis B, Kors N, Schellekens M, and van Rooijen N (1988) Effect of chronic injection of sphingomyelin-containing liposomes on lymphoid and non-lymphoid cells in the spleen. Transient suppression of marginal zone macrophages. *Br J Exp Pathol* **69**:865–875.

Dams ETM, Laverman P, Oyen WJG, Storm G, Scherphof GL, van der Meer JWM, Corsten FHM, and Boerman OC (2000) Accelerated blood clearance and altered biodistribution of repeated injections of sterically stabilized liposomes. *J Pharmacol Exp Ther* **292**:1071–1079.

Dijkstra J, van Galen M, Regts D, and Scherphof G (1985) Uptake and processing of liposomal phospholipids by Kuppfer cells in vitro. *Eur J Biochem* **148**:391–397.

Djordjevich L, Mayoral J, Miller IF, and Ivankovich AD (1987) Cardiorespiratory effects of exchanging transfusions with synthetic erythrocytes in rats. *Crit Care Med* **15**:318–323.

Fielding RM, Moon-Mcdermott L, Lewis RO, and Horner MJ (1999) Pharmacokinetics and urinary excretion of amikacin in low-clearance unilamellar liposomes after a single or repeated intravenous administration in the rhesus monkey. *Antimicrob Agents Chemother* **43**:503–509.

Gabizon A, Shmeeda H, and Barenholz Y (2003) Pharmacokinetics of pegylated liposomal Doxorubicin: review of animal and human studies. *Clin Pharmacokinet* **42**:419–436.

Goda N, Suzuki K, Naito S, Takeoka S, Tsuchida E, Ishimura Y, Tamatani T, and Suematsu M (1998) Distribution of heme oxygenase isoform in rat liver: topographic basis for carbon monoxide-mediated microvascular relaxation. *J Clin Investig* **101**:604–612.

Hamilton RG, Kelly N, Gawryl MS, and Rentko VT (2001) Absence of immunopathology associated with repeated IV administration of bovine Hb-based oxygen carrier in dogs. *Transfusion* **41**:219–225.

Hirano K, Kobayashi T, Watanabe T, Yamamoto T, Hasegawa G, Hatakeyama K, Suematsu M, and Naito M (2001) Role of heme oxygenase-1 and Kupffer cells in the production of bilirubin in the rat liver. *Arch Histol Cytol* **64**:169–178.

Hofbauer B, Friess H, Weber A, Baczako, Kisling P, Schilling M, Uhl W, Dervenis C, and Buchler MW (1996) Hyperlipaemia intensifies the course of acute oedematous and acute necrotising pancreatitis in the rat. *Gut* **38**:753–758.

Ishida T, Maeda R, Ichihara M, Irimura K, and Kiwada H (2003) Accelerated clearance of PEGylated liposomes in rats after repeated infusion. *J Controlled Release* **88**:35–42.

Izumi Y, Sakai H, Hamada K, Takeoka S, Yamahata T, Kato R, Nishide H, Tsuchida E, and Kobayashi K (1997) Physiologic responses to exchange transfusion with hemoglobin vesicles as an artificial oxygen carrier in anesthetized rats: changes in mean arterial pressure and renal cortical tissue oxygen tension. *Crit Care Med* **24**:1869–1873.

Kuipers F, Spanjer HH, Havinga R, Scherphof GL, and Vonk RJ (1986) Lipoproteins and liposomes as in vivo cholesterol vehicles in the rat: preferential use of cholesterol carried by small unilamellar liposomes for the formation of muricholic acids. *Biochim Biophys Acta* **876**:559–566.

Kyokane T, Norimuzu S, Taniai H, Yamaguchi T, Takeoka S, Tsuchida E, Naito M, Nimura Y, Ishimura Y, and Suematsu M (2001) Carbon monoxide from heme catabolism protects against hepatobiliary dysfunction in endotoxin-treated rat liver. *Gastroenterology* **120**:1227–1240.

Landaw SA (1988) Factors that accelerate or retard red blood cell senescence. *Blood Cells* **14**:47–59.

Laverman P, Carstens MG, Boerman OC, Dams ETM, Oyen WJG, Rooijen NV, Corstens FHM, and Storm G (2001) Factors affecting the accelerated blood clearance of polyethylene glycol-liposomes on repeated injection. *J Pharmacol Exp Ther* **298**:607–612.

Lian T and Ho RJY (2001) Trends and developments in liposome drug delivery systems. *J Pharm Sci* **90**:667–680.

O'Connell MJ, Ward RJ, Baum H, and Peters TJ (1989) Iron release from haemosiderin and ferritin by therapeutic and physiological chelators. *Biochem J* **260**:903–907.

Phillips WT, Klipper RW, Awasthi VD, Rudolph AS, Cliff R, Kwasiborski V, and Goins BA (1999) Polyethylene glycol-modified liposome-encapsulated hemoglobin: a long circulating red cell substitute. *J Pharmacol Exp Ther* **288**:665–670.

Rowland RN and Woodley JF (1980) The stability of liposomes in vivo to pH, bile salts and pancreatic lipase. *Biochim Biophys Acta* **620**:400–409.

Rudolph AS, Spielberg H, Spargo BJ, and Kossovsky N (1995) Histopathologic study following administration of liposome-encapsulated hemoglobin in the normovolemic rat. *J Biomed Mater Res* **29**:189–196.

Sakai H, Hara H, Yuasa M, Tsai AG, Takeoka S, Tsuchida E, and Intaglietta M (2000a) Molecular dimensions of Hb-based O_2 carriers determine constriction of resistance arteries and hypertension in conscious hamster model. *Am J Physiol* **279**:H908–H915.

Sakai H, Hisamoto S, Fukutomi I, Sou K, Takeoka S, and Tsuchida E (2004a) Detection of lipopolysaccharide in hemoglobin-vesicles by *Limulus* amebocyte lysate test with kinetic-turbidimetric gel clotting analysis and pretreatment with a surfactant. *J Pharm Sci* **93**:310–321.

Sakai H, Horinouchi H, Masada Y, Takeoka S, Kobayashi K, and Tsuchida E (2004b) Metabolism of hemoglobin-vesicles (artificial oxygen carriers) and their influence on organ functions in a rat model. *Biomaterials* **25**:4317–4325.

Sakai H, Horinouchi H, Tomiyama K, Ikeda E, Takeoka S, Kobayashi K, and Tsuchida E (2001) Hemoglobin-vesicles as oxygen carriers: influence on phagocytic activity and histopathological changes in metabolism. *Am J Pathol* **159**:1079–1088.

Sakai H, Masada Y, Horinouchi H, Yamamoto M, Ikeda E, Takeoka S, Kobayashi K, and Tsuchida E (2004c) Hemoglobin-vesicles suspended in recombinant human serum albumin for resuscitation from hemorrhagic shock in anesthetized rats. *Crit Care Med* **32**:539–545.

Sakai H, Tomiyama K, Masada Y, Takeoka S, Horinouchi H, Kobayashi K, and Tsuchida E (2003) Pretreatment of serum containing Hb-vesicles (oxygen carriers) to avoid their interference in laboratory tests. *Clin Chem Lab Med* **41**:222–231.

Sakai H, Tomiyama K, Sou K, Takeoka S, and Tsuchida E (2000b) Polyethyleneglycol-conjugation and deoxygenation enable long-term preservation of hemoglobin-vesicles as O_2 carriers in a liquid state. *Bioconjug Chem* **11**:425–432.

Sakai H, Tsai AG, Kerger H, Takeoka S, Tsuchida E, and Intaglietta M (1998)

Subcutaneous microvascular responses to hemodilution with a red cell substitute consisting of polyethyleneglycol-modified vesicles encapsulating hemoglobin. *J Biomed Mater Res* 40:66–78.

Sou K, Endo T, Takeoka S, and Tsuchida E (2000) Poly(ethylene glycol)-modification of the phospholipid vesicles by using the spontaneous incorporation of poly(ethylene glycol)-lipid into the vesicles. *Bioconjug Chem* 11:372–379.

Sou K, Naito Y, Endo T, Takeoka S, and Tsuchida E (2003) Effective encapsulation of proteins into size-controlled phospholipid vesicles using freeze-thawing and extrusion. *Biotechnol Prog* 19:1547–1552.

Stuecklin-Utsch A, Hasan C, Bode U, and Fleischhack G (2002) Pancreatic toxicity after liposomal amphotericin B. *Mycoses* 45:170–173.

Teicher BA, Ara G, Herbst R, Takeuchi H, Keyes S, and Northey D (1997) PEG-hemoglobin: effects on tumor oxygenation and response to chemotherapy. *In Vivo* 11:301–311.

Verkade HJ, Derksen JT, Gerding A, Scherphof GL, Vonk RJ, and Kuipers F (1991) Differential hepatic processing and biliary secretion of head-group and acyl chains of liposomal phosphatidylcholines. *Biochem J* 275:139–144.

Address correspondence to: Prof. Eishun Tsuchida, Advanced Research Institute for Science and Engineering, Waseda University, Tokyo 169-8555, Japan. E-mail: eishun@waseda.jp

Reduction of Methemoglobin via Electron Transfer from Photoreduced Flavin: Restoration of O_2-Binding of Concentrated Hemoglobin Solution Coencapsulated in Phospholipid Vesicles

Hiromi Sakai, Yohei Masada, Hiroto Onuma, Shinji Takeoka, and Eishun Tsuchida*

Advanced Research Institute for Science and Engineering, Waseda University, Tokyo 169-8555, Japan. Received April 9, 2004; Revised Manuscript Received July 31, 2004

Ferric methemoglobin is reduced to its ferrous form by photoirradiation either by direct photoexcitation of the heme portion to induce electron transfer from the surrounding media (Sakai at al. (2000) *Biochemistry 39*, 14595–14602) or by an indirect electron transfer from a photochemically reduced electron mediator such as flavin. In this research, we studied the mechanism and optimal condition that facilitates photoreduction of flavin mononucleotide (FMN) to $FMNH_2$ by irradiation of visible light, and the succeeding reduction of concentrated metHb in phospholipid vesicles to restore its O_2 binding ability. Visible light irradiation (435 nm) of a metHb solution containing FMN and an electron donor such as EDTA showed a significantly fast reduction to ferrous Hb with a quantum yield (Φ) of 0.17, that is higher than the method of direct photoexcitation of heme ($\Phi = 0.006$). Electron transfer from a donor molecule to metHb via FMN was completed within 30 ns. Native-PAGE and IEF electrophoresis indicated no chemical modification of the surface of the reduced Hb. Coencapsulation of concentrated Hb solution (35 g/dL) and the FMN/EDTA system in vesicles covered with a phospholipid bilayer membrane (Hb-vesicles, HbV, diameter: 250 nm) facilitated the metHb photoreduction even under aerobic conditions, and the reduced HbV restored the reversible O_2 binding property. A concentrated HbV suspension ([Hb] = 8 g/dL) was sandwiched with two glass plates to form a liquid layer with the thickness of about 10 μm (close to capillary diameter in tissue, 5 μm), and visible light irradiation (221 mW/cm^2) completed 100% metHb photoreduction within 20 s. The photoreduced $FMNH_2$ reacted with O_2 to produce H_2O_2, which was detected by the fluorescence measurement of the reaction of H_2O_2 and *p*-nitrophenylacetic acid. However, the amount of H_2O_2 generated during the photoreduction of HbV was significantly reduced in comparison with the homogeneous Hb solution, indicating that the photoreduced $FMNH_2$ was effectively consumed during the metHb reduction in a highly concentrated condition inside the HbV nanoparticles.

INTRODUCTION

Photoinduced electron transfer is an essential reaction in biological systems especially during photosynthesis by the chlorophyll–protein complex (*1*). Hemoproteins such as hemoglobin (Hb) and myoglobin (Mb) are originally not related to the photoreaction in a biological system; however, photoexcitation and the resulting electron transfer reactions have been extensively studied (*2–6*). In our previous report, we clarified the mechanism of reduction of ferric methemoglobin (metHb) to its ferrous form by the direct excitation of the porphyrin N band in the UVA region (*7*). The reduction proceeds by charge transfer from the porphyrin ring to the central ferric iron to form the porphyrin π cation radical and ferrous iron by the N band excitation, and the contribution of the amino acid residues in the globin chain as an electron donor or an electron pathway. Another photochemical process to reduce metHb is an electron transfer from photochemically reduced flavin derivatives. The precise photoreduction mechanism of a flavin derivative to its reduced form has been extensively studied (*8–10*), and this has contributed to the understanding of the mechanism of the electron transfer of flavoproteins (*11–17*) and their function in the biological systems such as bacterial photosynthesis (*18*) and visual organs (*19*). Irrespective of the flavoproteins, the photoreduction of metMb and metHb by the externally added photoreduced form of the flavin mononucleotide (FMN) was first reported by Brwon and Synder (*20*) and Yubisui et al. (*21*, *22*), respectively.

We have paid special attention to the reduction of hemoproteins that will be applicable to Hb-based artificial red cells (*23*). We focus on the liposome-encapsulated Hb; a concentrated Hb solution is encapsulated in phospholipid vesicles to form Hb-vesicles (HbV)[1] with a particle size of about 250 nm (*24*, *25*). Ferrous state Hb binds oxygen to form HbO_2; however, it gradually converts to ferric metHb and superoxide anion and loses its oxygen binding property both in vivo and in vitro (*26*). A series of thiols was studied as a reductant for metHb,

* To whom correspondence should be addressed. Phone, +81-3-5286-3120; Fax, +81-3-3205-4740; e-mail, eishun@waseda.jp.

[1] Abbreviations: HbV, Hb-vesicles; FMN, flavin mononucleotide; SOD, superoxide dismutase; EDTA, ethylenediamine tetraacetic acid; DTPA, diethylenetriamine pentaacetic acid; IEF, isoelectric focusing; Native-PAGE, Native-polyacrylamide gel electrophoresis; PEG, poly(ethylene glycol); DPPC, 1,2-dipalmitoyl-*sn*-glycero-3-phosphatidylcholine; DHSG, 1,5-*O*-dihexadecyl-*N*-succinyl-L-glutamate; PEG-DSPE, 1,2-distearoyl-*sn*-glycero-3-phosphatidylethanolamine-*N*-PEG_{5000}; HbCO, carbonylhemoglobin; $[FMN]_{in}$, concentration of FMN in HbV; $[EDTA]_{in}$, concentration of EDTA in HbV; $[heme]_{in}$, concentration of heme in HbV; PHA, *p*-hydroxyphenylacetic acid; DBDA, 6,6′-dihydroxy-(1,1′-biphenyl)-3,3′-diacetic acid, FMN*, triplet FMN; $FMNH_2$, reduced form of FMN;

10.1021/bc049913z CCC: $27.50
Published on Web 08/26/2004

which is coencapsulated in the vesicles (*27, 28*). As a result, the functional half-life of the Hb-vesicles is doubled by coencapsulation of the DL-homocysteine and active oxygen scavengers (*27, 29*). To retard metHb formation, bioconjugation of enzymes such as catalase or superoxide dismutase (SOD) (*30*) and coencapsulation of RBC enzymes including the metHb reductase system, carbonic anhydrase, SOD, or catalase (*29, 31*) have also been reported.

To restore the O_2 binding property of HbV, we tested utilization of the photoreduction system: the indirect excitation of an externally added electron mediator (*32*), or the direct excitation of metHb absorption in the UV region (*7*). In this study, we have made significant efforts to find out a condition that facilitates metHb reduction by a photoreduced flavin mononucleotide (FMN), because this system was well characterized by Everse (*32*), and the advantages of this system are visible light irradiation and high quantum yield (*9, 10*). We analyzed the influence of electron donors to FMN, dissolved gases, etc., to find the facilitating condition and elucidate the mechanism for the facilitation of the metHb photoreduction in the HbV nanoparticles, a structure similar to that in red blood cells (RBCs), and this may also help understand the underlying mechanism of the reaction of NADPH-flavin reductase and metHb in RBCs.

EXPERIMENTAL PROCEDURES

Preparation of metHb. Carbonylhemoglobin (HbCO) was purified from outdated donated blood offered by the Hokkaido Red Cross Blood Center as previously reported (*33, 34*). MetHb was prepared by reacting HbCO with an excess amount of potassium ferricyanide. The unreacted ions and ferrocyanide ions were removed twice by stirring with a mixed bed ion-exchange resin (Bio Rad AG 501-X8), and the solution was then permeated through 0.22 μm-filters (Advantec Co.). The metHb conversion was 99.8% measured by the cyanomethemoglobin method.

Chemicals. Amino acids (Met, Gln, Arg, Glu, Phe, Lys, Tyr, and Trp) were purchased from the Kanto Chem. Co (Tokyo). Peptides (Met-Met and Met-Gly) were from Sigma, and saccharides (mannitol, maltotriose, dextran, glucoseamine, glucron amide), methanol, citric acid sodium salt, ethylenediamine tetraacetic acid (EDTA), and diethylenetriamine pentaacetic acid (DTPA) were from the Kanto Chem. Co. All the chemicals were used without purification.

Photoreduction of FMN in the Presence of an Electron Donor. Three milliliters of phosphate-buffered saline (10 mM PBS, pH 7.4) with an electron donor (e.g., amino acids, peptides, sugars, as listed above, 20 mM) was sealed in a cuvette (2 mm width) with a butyl rubber cap. The solution was bubbled with N_2 for 30 min. A stock solution of FMN prepared in the dark was added at a concentration of 10 μM. The light source was a super high-pressure mercury lamp (USH-250D, 250W, Ushio Co., Tokyo) with a cutoff filter (L-42 and HA-50, Hoya Co., Tokyo) to obtain a single beam with the maximum wavelength of about 435 nm, which is close to λ_{max} of FMN (450 nm). The cuvette was located 2.5 cm away from the light source, and the light intensity was 221 mW/cm^2 that was measured with a power meter (PSV-3102, Gentec Co.). The conversion of the reduction, FMN to $FMNH_2$, was calculated from the reduction of absorbance at 450 nm, measured with an UV/vis spectrophotometer (V-560, Jasco, Tokyo).

Photoreduction of metHb in the Presence of FMN and an Electron Donor. Three milliliters of phosphate-buffered saline (10 mM PBS, pH 7.4) with an electron donor and FMN was sealed in a cuvette (2 mm width) with a butyl rubber cap. The solution was bubbled with N_2 gas for 30 min. A concentrated metHb stock solution deaerated by a gentle N_2 flowing in another bottle (about 3 mM, 10 μL) was injected into the cuvette. This procedure avoided bubbling of a metHb solution that might induce foaming and metHb denaturation. The final concentration of heme was 0.1 mM. The cuvette was exposed to the same visible light (435 nm) as described above. The conversion of the metHb reduction was calculated from the ratio of the Soret band absorption at 405 nm (λ_{max} of metHb) versus 430 nm (deoxyHb) or 415 nm (HbO_2).

A laser flash photolysis system (Tokyo Instr. Co.) was used for the transient spectrum measurement of the reduction of FMN and the succeeding metHb (*7*). The sample solutions were excited at 450 nm with a Pulsed Nd:YAG laser (SL803G-10, Spectron Laser Systems, Ltd.) equipped with an optical parametric oscillator. One irradiation time was 5–8 ns (fwhm) and the interval was 100 ms. A total of 100 accumulations were collected to get an acceptable signal-to-noise ratio. The transient spectra were recorded between 350 and 550 nm using a spectrophotometer (MS257, Oliel Instr. Co.) equipped with an ICCD detector (DH520–18F–WR, ANDOR Technol. Co.). A sample solution was placed in a 10 mm quartz cuvette and purged with N_2. The fastest time point of the measurements was 30 ns. A solution of FMN (100 μM)/Met (20 mM) in a 10 mM phosphate-buffered saline (pH 7.4), and a solution of FMN (5 μM)/Met (20 mM)/metHb ([heme] = 10 μM) in the phosphate-buffered saline were tested.

Quantum Yield Measurement. The ferrioxalate actinometer of $K_3[Fe(C_2O_4)_3]\cdot 3H_2O$ was used to measure the quantum yield (Φ) of metHb photoreduction (*7, 35, 36*). In the actinometer, Φ of the photoreduction of Fe^{3+} to Fe^{2+} was assumed to be 1.11 (*35*), and this value was used to calculate the total photons absorbed by the sample solution and Φ of the metHb photoreductions.

Isoelectric Focusing (IEF) and Native Polyacrylaminde Gel Electrophoresis (Native-PAGE). IEF and native-PAGE were performed on PhastGel IEF 3–9 (pH 3–9) and PhastGel Gradient 8–25 (PAGE content, 8–25%) (Amersham Pharmacia Biotech), respectively, with the PhastSystem (Pharmacia). The photoreduced Hbs in N_2 and air in the presence of FMN/EDTA was compared with metHb and the purified HbO_2.

IEF. Forty microliters of sample (1 mg/mL) per one lane was applied on the gel. This was focused and then stained with PhastGel Blue R (Coomassie brilliant blue) in the development unit of the PhastSystem. The marker was the p*I* calibration kit 3–10 (Pharmacia).

Native-PAGE. The samples were applied on the gel and the electrophoresis was automatically performed. The gel was stained with PhastGel Blue R. The marker was HMW Kit E (Parmacia).

Restoration of Oxygen Binding Property. The photoreduced deoxyHb solution ([heme] = 20 mM, [FMN] = 5 μM, [EDTA] = 10 mM) in an Ar atmosphere was bubbled with oxygen, and the UV/vis spectroscopy was measured. The photoreduced Hb solution was permeated through a column of Sephadex G-25 (Pharmacia) to remove FMN, the oxygen equilibrium curve of the obtained Hb solution was obtained at 37 °C with a Hemox Analyzer (TCS Products Inc.), and the oxygen affinity (P_{50}) and Hill number were measured. The Hb samples were diluted in a Hemox phosphate buffer (TCS Products Inc.).

Preparation of Hb-Vesicles Coencapsulating FMN and EDTA, and the Photoreduction of metHb. HbVs were prepared as previously reported (*24*, *34*, *37*). The purified HbO_2 solution (35 g/dL, [heme] = 21.7 mM) contained FMN (5, 10, or 50 mM) and EDTA (10, 20, 30, 50, or 200 mM), this was mixed with the lipid mixtures, and the resulting multilamellar vesicles were extruded through filters to regulate the vesicular size. The lipid bilayer was composed of a mixture of 1,2-dipalmitoyl-*sn*-glycero-3-phosphatidylcholine (DPPC), cholesterol, and 1,5-*O*-dihexadecyl-*N*-succinyl-L-glutamate (DHSG) at the molar ratio of 5/5/1 (Nippon Fine Chem. Co., Osaka), and 1,2-distearoyl-*sn*-glycero-3-phosphatidylethanolamine-*N*-PEG_{5000} (PEG-DSPE, NOF Co., Tokyo) (*38*). Thus the vesicular surface was covered with PEG chains. The molar composition of the DPPC/cholesterol/DHSG/PEG-DSPE was 5/5/1/0.033. HbVs were suspended in a physiologic salt solution at [Hb] = 10 g/dL. The suspension was incubated in the dark at 40 °C for 48 h to facilitate the metHb formation and to prepare metHbV. The concentrations of FMN, EDTA, and heme of Hb in HbV, expressed as $[FMN]_{in}$, $[EDTA]_{in}$, and $[heme]_{in}$, respectively, are assumed to be identical to the fed concentrations for the HbV preparation.

Photoreduction of metHbV was performed in the same manner with a metHb solution in a relatively diluted condition ([heme] = 10 μM) in a 2 mm quartz cuvette. At a higher concentration ([heme] = 5 mM) under aerobic condition, the suspension of metHbV was sandwiched between two glass plates. The optical path length was 10 μm.

Measurement of H_2O_2 in the metHb Photoreduction. The reaction of *p*-hydroxyphenyl acetic acid (PHA) and H_2O_2 to generate a fluorescent dimer, 6,6'-dihydroxy (1,1'-biphenyl)-3,3'-diacetic acid (DBDA), was used to detect H_2O_2 generated during the metHb photoreduction in the metHbV and metHb solutions. During the photoreduction of metHb or metHbV ([heme] = 20 μM in a cuvette) in the presence of FMN (5 μM)/EDTA (50 μM), 1 mL of sample was pipetted out and immediately mixed with horseradish peroxidase (Sigma, 3.7 μM), and PHA (5.8 mM). The mixture was ultracentrifuged in a tube with a filter (Cut off Mw. 30 kDa, Ultrafree, Amicon) at 12 000 rpm for 20 min to remove Hb or HbV and to obtain the filtrate solution. The fluorescence of the filtrate was measured with a fluorometer (JASCO, Ex: 317 nm, Em: 404 nm). The calibration curve was obtained by analysis of a diluted standard H_2O_2 solution (Kanto Chem., Co).

RESULTS

Photoreduction of FMN with an Electron Donor. Figure 1 shows the time course of the conversion of FMN to $FMNH_2$ by irradiation of visible light (435 nm). FMN primarily converts to the photoexcited triplet FMN* and this reacts with two electron donors (D) to generate $FMNH_2$. The reduction can be confirmed by the decrease in the absorption of the characteristics peaks at 370 and 450 nm. Without an addition of an electron donor, photoreduction gradually proceeds (baseline, initial reduction rate = 12 μM/min) (Table 1). A ribityl group in a FMN molecule of itself can be an electron donor. However, further irradiation should induce decomposition that was evident from the phenomena that the spectroscopic curves did not coincide at the isosbestic point. A significantly fast reduction was observed by the addition of EDTA and DTPA that were 88 and 84 times faster than the condition without the addition of an electron donor. Among the amino acids, Met showed the fastest

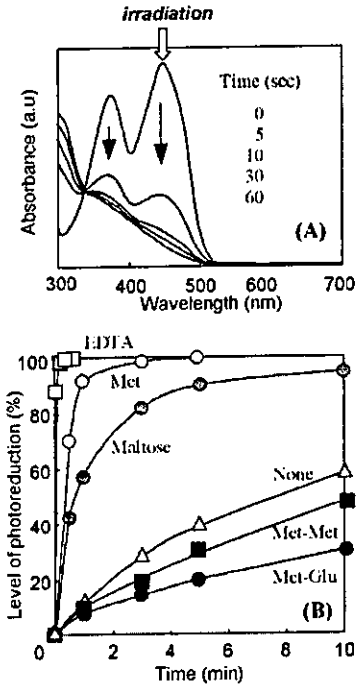

Figure 1. (A) Time course of the spectral changes during the conversion of FMN to $FMNH_2$ in the presence of EDTA (20 mM) by visible light irradiation (435 nm). The characteristic two peaks disappeared with the photoreduction conversion. (B) Time course of the conversion of FMN to $FMNH_2$ with various electron donors. EDTA and Met showed fast photoreduction rate. On the other hand, Met-Met and Met-Glu retarded the reaction. [FMN] = 100 μM, [electron donor] = 20 mM, pH = 7.4, in N_2 atmosphere.

Table 1. Initial Rates of the Photoreduction of FMN to $FMNH_2$ with Various Electron Donors (10 mM)

electron donor	mw	initial reduction rate (μM/min)	comparison with baseline
EDTA	292	1056	88
DTPA	393	1008	84
Met	149	140	11.7
Met-Met (10 mM)	280	5	0.2
Met-Met (20 mM)	280	10	0.8
Met-Glu	278	7	0.6
Arg	174	124	10.3
Phe	165	118	9.8
Lys	146	104	8.7
Gln	146	58	4.8
Glu	147	46	3.8
mannitol	182	45	3.8
maltotriose (10 unit mM)	504	47	3.9
dextran (10 unit mM)	5×10^6	45	3.6
glucoseamine	216	100	8.3
glucron amide	193	72	6.0
methanol	32	42	3.5
citric acid sodium salt	294	40	3.3
hydrogen	2	82	6.8
none (baseline)	---	12	1.0

reduction rate (140 μM/min, 12 times faster than the baseline), while Arg, Phe, Lys, Glu, and Gln showed moderate facilitation. On the other hand, Tyr and Trp showed slower rates of photoreduction. Unexpectedly, Met-Met and Met-Glu lowered the reduction rate. As for the saccharides, mannitol, maltotriose, dextran, glucosamine, and glucron amide showed similar facilitation at the same glucose units. However, they are much slower than Met and EDTA. The presence of H_2 gas

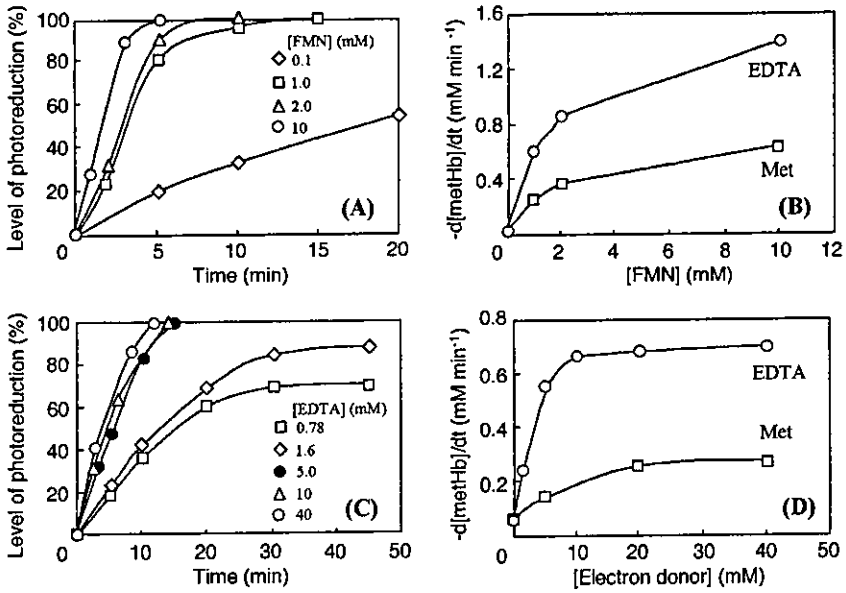

Figure 2. Influence of the concentrations of FMN and EDTA on the rate of metHb reduction. The time course of the level of photoreduction and the initial reaction rates are summarized. (A, B): Influence of the FMN concentration at a constant [EDTA] (20 mM). [FMN] was at 0.1, 1.0, 2.0, or 10 mM. (C, D): Influence of [EDTA] at the constant [FMN] (1.0 mM). [EDTA] was at 0.78, 1.6, 5.0, 10, or 40 mM. The data for the Met addition were inserted as a reference. [heme] = 3.1 mM.

slightly facilitated the reduction. Citric acid and methanol showed a slight facilitation. From these results, EDTA and Met were mainly studied as electron donors.

Reduction of metHb by the Photoreduced FMNH$_2$. The reduction of metHb by the photoreduced $FMNH_2$ was evident from the spectroscopic change of λ_{max} in the Soret and Q-bands. The influence of the concentration of FMN was examined at constant concentrations of metHb (5 g/dL, [heme] = 3.1 mM) and EDTA (20 mM) (Figure 2A). The presence of 100 μM FMN showed 50% reduction of metHb at 20 min; however, 1 mM FMN completed the reduction at 15 min. The influence of the EDTA concentration was examined at constant concentrations of metHb ([heme] = 3.1 mM) and FMN (1.0 mM) (Figure 2B). Without EDTA, the metHb photoreduction proceeded since a ribityl group of FMN and probably globin of Hb can be an electron donor. When the EDTA concentration was less than that of the heme concentration, the reduction rate was very slow, and the reduction could not be completed. However, 5 mM EDTA and higher showed a faster rate and the reduction was completed within 15 min. Similar results were obtained with Met; however, the initial rates were much slower than with EDTA.

The transient spectrum of the photoreduction of FMN in the presence of Met after laser flash irradiation showed the reduction of the absorbances at 445 and 373 nm at 30 ns, and the spectral profile was the same at 5 ms (data not shown here). Therefore, the photoreduction of FMN to $FMNH_2$ was completed within 30 ns. In the presence of metHb, a total of 30 ns was enough to observe the reduced deoxyHb (λ_{max} = 430 nm) and the spectrum was the same for 5 ms.

The influence of the presence of O_2 was examined (Figure 3). The metHb photoreduction in the presence of EDTA and FMN in the N_2 atmosphere completed the reduction within 15 min. The metHb photoreduction under the aerobic conditions became slightly slower, and the level of reduction reached 95% and then showed a plateau. In the case of the addition of Met, the reduction was completed within 40 min in the N_2 atmosphere that

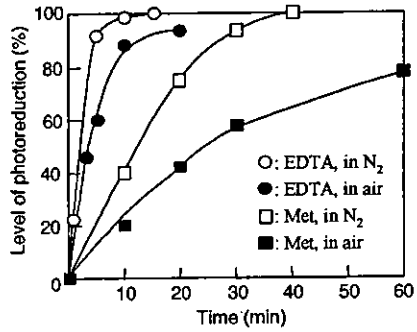

Figure 3. The influence of the presence of O_2 on the rate of photoreduction of metHb ([heme] = 3.1 mM) with FMN (1.0 mM) and an electron donor (20 mM) at pH 7.4. The data for Met addition (1.0 mM) were also inserted as a reference. The presence of O_2 retarded the metHb photoreduction.

was much slower in comparison with the EDTA addition. Under the aerobic condition, the reduction in the presence of Met was significantly slow and did not reach 80% at 60 min.

Native-PAGE of the photoreduced Hb both in the N_2 and aerobic atmospheres showed identical bands with the normal oxyHb and meHb (Figure 4A). Even though the Mw of Hb is 64.5 kDa, it showed a higher relative Mw than albumin (67 kDa) as one of the markers in the Native-PAGE in the absence of sodium dodecyl sulfate, SDS, because the surface charge of the protein directly affect on the traveling distance during the electrophoresis. IEF of the photoreduced Hbs showed the presence of HbO_2 at pI = 7.0 as a dense band and a weak band at pI = 7.2 of a partially reduced Hb (Figure 4B). There was no band at 7.4 that corresponds to metHb.

The oxygen dissociation curve of the photoreduced Hb was identical with that of the normal HbO_2 (Data not shown here). The P_{50} and Hill number of the photoreduced Hb were 10.5 Torr and 1.8, respectively, and they were almost identical with the normal HbO_2 (11 Torr and 1.7, respectively).

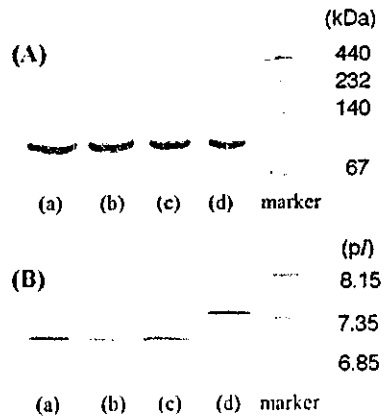

Figure 4. Native-PAGE (A) and IEF (B) of the photoreduced Hb in the presence of EDTA and FMN both in N_2 and aerobic atmospheres: (a) photoreduced Hb in N_2, (b) photoreduced Hb in air, (c) oxyHb, (d) metHb. In A, there was no change in the molecular weight of the Hb subunits. Since Native-PAGE does not include sodium dodecyl sulfate, the surface property of the protein directly affect on the traveling distance during electrophoresis. Therefore, Mw of Hb (Mw = 64.5 kDa) seemed much larger than albumin marker (Mw = 67 kDa). In B, the band at 7.4, which corresponded to metHb, almost disappeared in lanes a and b. No other bands were observed.

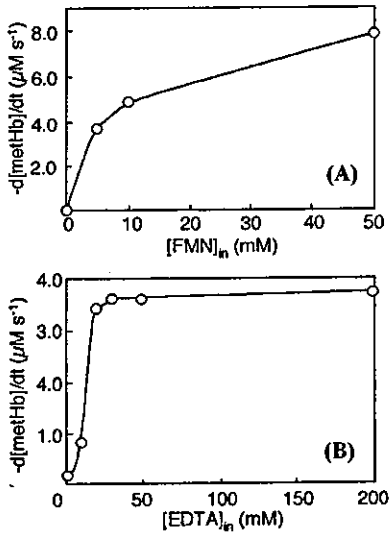

Figure 5. Influence of the concentrations of FMN and EDTA inside HbV on the initial rate of metHb reduction. (A) Influence of $[FMN]_{in}$ at the constant $[EDTA]_{in}$ = 20 mM. (B) Influence of $[EDTA]_{in}$ at the constant $[FMN]_{in}$ = 5 mM. [heme] = 10 μM in the cuvette, $[heme]_{in}$ = 21.7 mM. When $[EDTA]_{in}$ was higher than $[heme]_{in}$, the initial rate of metHb reduction was plateau.

Reduction of metHb in Hb-Vesicles. At first a diluted metHbV suspension ([heme] = 10 μM in a cuvette; $[heme]_{in}$ = 21.7 mM) was tested for photoreduction to analyze the kinetics. The initial rate of metHb reduction increased with increasing $[FMN]_{in}$ at a constant $[EDTA]_{in}$ (20 mM); however, the initial rate at $[FMN]_{in}$ = 10 mM was lower than twice that at $[FMN]_{in}$ = 5 mM (Figure 5A). At a constant $[FMN]_{in}$ (5 mM), increasing the $[EDTA]_{in}$ significantly facilitated the metHb photoreduction, however, the photoreduction rate did not increase above 20 mM (Figure 5B). This critical concentration is almost identical to $[heme]_{in}$ (21.7 mM). From these results, the rate-determining step of this system should be the electron transfer from an electron donor to the photoexcited FMN.

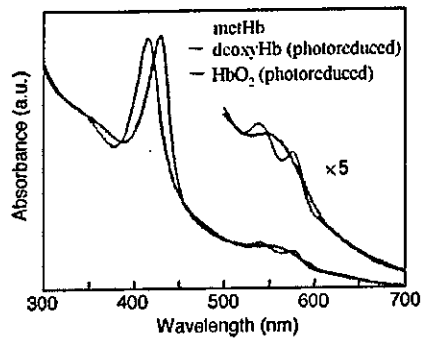

Figure 6. UV–visible spectra of HbV before irradiation (metHb), after photoreduction (deoxyHb), and its oxygenated form (HbO_2). $[EDTA]_{in}$ = 50 mM, $[FMN]_{in}$ = 5 mM, $[heme]_{in}$ = 21.7 mM. These spectra indicate the successful restoration of O_2-binding property of HbV.

The absorption spectra of the metHbV and the photoreduced HbV (λ_{max} = 430 nm) are shown in Figure 6. Due to the light scattering effect of the HbV particles, the turbidity was higher at a lower wavelength (*39*). Bubbling with an O_2 gas in a photoreduced HbV solution reversibly converted deoxyHb to HbO_2 with a characteristic shift of λ_{max} from 430 to 415 nm, indicating that the oxygen binding ability was successfully restored.

The concentration of [heme] in an HbV suspension for the intravenous infusion should be estimated to about 3–6 mM, which is significantly higher in comparison with 10 μM in a cuvette for the absorption spectral analysis. To test the photoreduction at a practical Hb concentration, a metHbV suspension ([heme] = 5.0 mM) was sandwiched between two glass plates and irradiated with visible light. The photoreduction proceeded quite promptly (Figure 7). Due to the thin liquid layer (ca. 10 μm in thickness), the effect of light scattering seen in Figure 6 is minimized. At the constant $[FMN]_{in}$ (5 mM) condition, the $[EDTA]_{in}$ of 10 and 20 mM were not enough to complete the reduction. At $[EDTA]_{in}$ = 50 mM, the photoreduction was significantly fast and the reaction was completed within 20 s with the characteristic λ_{max} of deoxyHb (430 nm). At $[FMN]_{in}$ = 100 mM and $[EDTA]_{in}$ = 20 mM, the initial reduction rate was the fastest; however, the reduction was not completed which was evident from the fact that the absorption at 430 nm in the Soret band was not high enough. The value of $[EDTA]_{in}$ should at least be higher than $[heme]_{in}$ (21.7 mM).

Quantum Yield of the Photoreduction Reactions. Table 2 summarizes the quantum yield, Φ, of various photoreduction conditions. The combination of metHb/FMN/EDTA showed the highest value (0.17) in an Ar atmosphere at [heme] = 0.1 mM. This was about 28 times higher than that for the photoreduction by the direct excitation of the N-band irradiating by near UV light (365 nm, Φ = 0.003–0.006) (*7*), and 4 times higher than the condition without an electron donor (0.04). In the case of HbV that coencapsulates FMN and EDTA, the concentrations of the components in the cuvette were much smaller, however, the concentrations in the nanoparticles (HbV) are much higher and the Φ for HbV was also very high (0.09–0.11). Probably due to the light scattering effect of HbV, Φ for HbV is slightly lower than that for the homogeneous Hb solution, but significantly higher than that for the N-band excitation (0.003–0.006).

Measurement of H_2O_2 in the metHb Photoreduction. Visible light irradiation to metHb([heme] = 20 μM)/FMN(5 μM)/EDTA(50 μM) under aerobic conditions

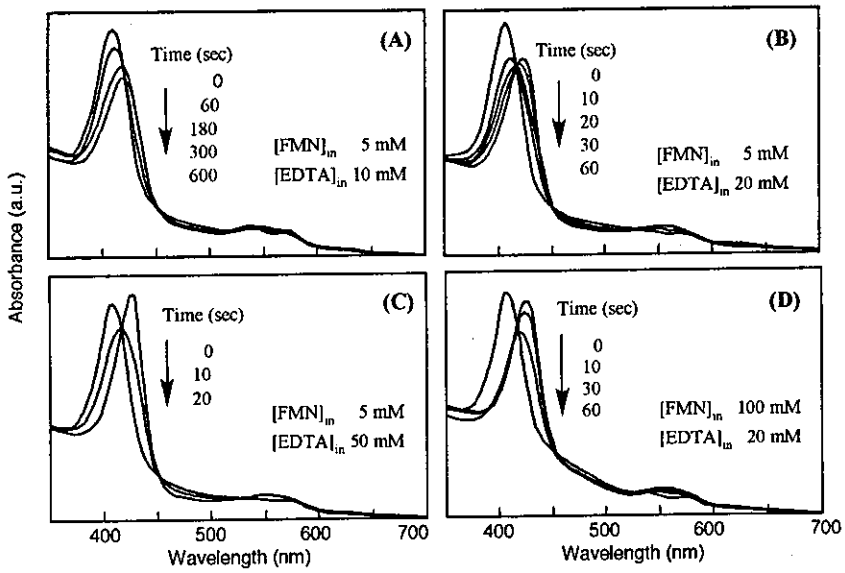

Figure 7. UV–visible spectral changes of HbV in a liquid layer sandwiched between two glass plates during photoreduction under aerobic conditions. The thickness of the layer was approximately 10 μm. Condition (C) ($[FMN]_{in}$ = 5 mM, $[EDTA]_{in}$ = 50 mM) showed the fastest rate of photoreduction, and the reaction was completed within 20 s. The arrows indicate the decrease in absorbance at 405 nm of MetHb with irradiation time.

Table 2. Quantum Yield (Φ) of Photoreduction of metHb and metHbV

	heme (mM)	FMN (mM)	electron donor (mM)	condition	λ_{ex} (nm)	Φ
metHb	0.1	0.01	EDTA (20)	in Ar	435	0.17
	0.1	0.01	Met (20)	in Ar	435	0.11
	0.1	0.01	no addition	in Ar	435	0.04
metHbV	0.01 (21.7)[a]	2.3×10^{-3} (5)[a]	EDTA (9.2×10^{-3}) (20)[a]	in Ar	435	0.09
	0.01 (21.7)[a]	46×10^{-3} (100)[a]	EDTA (9.2×10^{-3}) (20)[a]	in Ar	435	0.11
metHb	0.01	–	Trp (1.0)	in Ar	365	0.006[b]
	0.01	–	mannitol (100)	in CO	365	0.006[b]
	0.01	–	no addition	in CO	365	0.003[b]

[a] Concentrations of the components inside HbV; $[heme]_{in}$, $[FMN]_{in}$, $[EDTA]_{in}$. [b] Data from ref 7.

produced H_2O_2, and the fluorescent intensity of DBDA (λ_{em} = 404 nm) significantly increased (Figure 8a). The amount of H_2O_2 reached 40 μM at 120 s (Figure 8b). Irradiation to FMN alone produced 100 μM H_2O_2 for 120 s without any formation of $FMNH_2$. We confirmed that the irradiation to metHb alone did not produce H_2O_2 (data not shown here). The level of metHb photoreduction was less than 20% at 120 s (Figure 8c). A significant suppression of H_2O_2 generation was confirmed for the irradiation to metHbV and the H_2O_2 generation decreased to less than 20 μM, and the level of metHb photoreduction reached 50% at 120 s. A further increase in the level of photoreduction to 80% was confirmed when the partial oxygen pressure in the cuvette was regulated to 40 Torr; however, the amount of H_2O_2 could not be significantly reduced.

DISCUSSION

We found for the first time that the coencapsulation of concentrated Hb solution and the FMN/EDTA system in phospholipid vesicles (HbV) significantly facilitated the reduction of metHb by visible light irradiation (435 nm). This was evident from the Φ of the reaction, i.e., 0.17 for the Hb solution and 0.10 for the HbV suspension. The lowered Φ for HbV in comparison with that for a Hb solution is probably due to the light scattering of the illuminated visible light due to the particle of HbV (diameter, 250 nm) (*39*). However, they are much higher than that for the metHb photoreduction via direct photoexcitation of the N-band of the porphyrin ring in the UVA region (Φ = 0.006) (*7*). Even though the concentrations of the components in the cuvette were much lower for HbV than for the homogeneous Hb solution as shown in Table 2, the concentrations inside HbV were significantly higher and this condition facilitated the desired reactions (photoreduction of FMN and metHb) and suppressed the unwanted side reactions (generation of active oxygen species).

The reaction mechanism is that the photoexcited triplet FMN* rapidly receives an electron from the donor molecule, EDTA, to transform to the semiquinone followed by disproportionation to the two electron reduced form, $FMNH_2$. They are effective reducing agent to offer an electron to metHb. According to Yubisui et al., $FMNH_2$ reduces metHb with the rate constant of 5.5×10^6 M^{-1} s^{-1} (*22*), which is significantly faster than do glutathione (rate constant = 2.5×10^{-3} M^{-1} s^{-1}) (*27*) and ascorbic acid (3.0×10^{-3} M^{-1} s^{-1}) (*22*). The transient spectrum of the reduction of metHb by the photoreduced form of FMN demonstrated the completion of the reaction at 30 ns. Our result may be plausible because it is reported that a flavocytochrome showed complete photoreduction within 100 ns (*14*), measured by a laser flash-induced transient absorption difference spectra. The externally added FMN should more freely access to the protoporphyrin IX (heme) in the Hb molecule and would show a faster electron transfer. It is reported that the direct chemical conjugation of flavin to the propionic acid residue of heme significantly facilitates the electron transfer from flavin to heme in a reconstituted myoglobin (*40, 41*). Therefore,

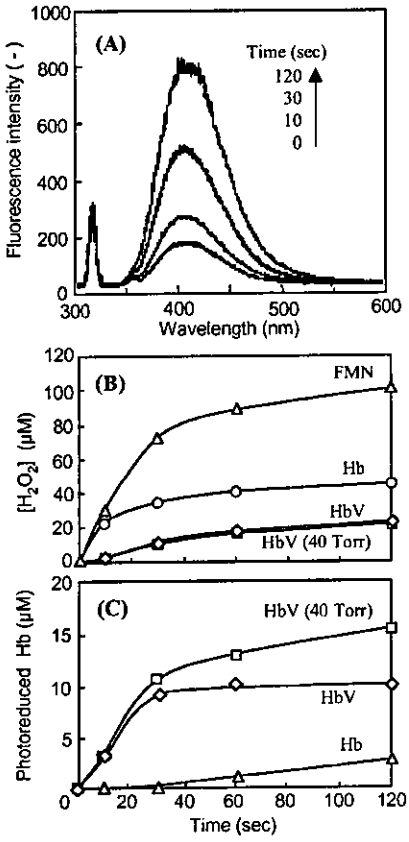

Figure 8. Detection of H_2O_2 using the fluorescence of DBDA during the photoreduction of Hb and HbV in the presence of FMN and EDTA. (A) An example of the fluorescence spectroscopy of the DBDA. The fluorescence intensity (λ_{em} = 404 nm) increased with time during the photoreduction of metHb solution under aerobic conditions (pO_2= 150 Torr). (B) Time course of the generation of H_2O_2 during the photoreduction of Hb and HbV under aerobic conditions (pO_2= 150 Torr), and HbV at pO_2 = 40 Torr. Irradiation to FMN alone was also tested as a reference (top curve) that produced 100 μM H_2O_2 for 120 s. Liberation of H_2O_2 from HbV was significantly suppressed in comparison with Hb solution. (C) The levels of metHb photoreduction during the measurement of H_2O_2 generation. The concentrations of heme (20 μM), FMN (5 μM), and EDTA (50 μM) in the cuvette were identical between the metHb solution and HbV suspension. For HbV, $[heme]_{in}$ = 21.6 mM, [FMN]in = 5 mM, and $[EDTA]_{in}$ = 50 mM.

two propionic acid groups of a heme that directly face the outer aqueous phase of an Hb molecule should contribute to the electron transfer from the externally added FMN to the heme.

The side reaction of $FMNH_2$ is the reaction with O_2 to generate singlet O_2 ($^1O_2$) or H_2O_2 (*11*, *42*), due to the low redox potential of reduced flavin (E_m = −209 mV). However, according to the quantitative measurement of H_2O_2, photoreduction of metHbV significantly reduced the side reaction in comparison with the metHb solution. This effect is due to the highly concentrated condition inside metHbV: the photoexcited FMN* readily reacts with EDTA to generate $FMNH_2$, and it also readily reacts with concentrated metHb inside the HbV nanoparticle. However, for the complete removal of H_2O_2, further coencapsulation of catalase would be effective (*29*) in the presence of O_2. Of course, in the absence of O_2, only the metHb reduction proceeds.

We tried to find other optimal electron donors instead of EDTA, because it has been reported that the oxidized and decomposed EDTA elements contain acetaldehyde that might react with the lysine residues on a protein molecule (*10*), and EDTA is a strong chelator of Ca^{2+} as an anticoagulant and may require caution when using a large dosage. We confirmed that Met was effective secondary to EDTA, as reported by other researchers (*9*, *32*). Arg was also effective, but it was not stable against oxidation during incubation under aerobic conditions at 37 °C for 3 days. Met was stable against oxidation. However, the small amino acid, Met (Mw = 149), gradually leaks out from the HbV across the phospholipid bilayer membrane (data not shown). To minimize the leakage of an electron donor, larger molecules, Met-Met and Met-Glu, were tested. Unexpectedly, they did not show any contribution as an electron donor and retarded the reduction of FMN. The ribityl phosphate group in the FMN molecule can be an electron donor, because the photoreduction of FMN proceeds without the addition of an electron donor. The retardation by the peptides should be probably due to some interaction of these peptides with the ribityl phosphate group that may hinder the electron transfer to the isoalloxazine ring. Other amino acids such as Phe and Lys, and saccharides such as mannitol or maltotoriose, are effective as an electron donor; however, their reduction rates of FMN were much lower in comparison with EDTA. Interestingly, methanol and gaseous H_2 also showed facilitation. DTPA, a structure similar to EDTA, showed an effectiveness comparable with EDTA. EDTA is a well-known electron donor, and its larger size (Mw = 292) and four negative charges prevent leakage from the vesicles. We could not find a more effective electron donor in our study, but confirmed that IEF and native-PAGE did not demonstrate any change in the chemical modification of the photoreduced Hb in the presence of EDTA/FMN, and the O_2 binding property was successfully restored. Therefore, we tested coencapsulation of FMN/EDTA in HbV for the other studies.

When HbV is intravenously infused for the substitution of blood, the concentrations of Hb and the heme of HbV in plasma should reach 5 g/dL and 3.1 mM, respectively, or higher (*43*). These are much higher than the experimental conditions in Figures 1−4, and it is impossible to test such a highly concentrated solution in a cuvette because of the strong light scattering by the particles and absorption by Hbs. We thus tested sandwiching the solution with two glass plates, thus making a thin liquid layer between the glass plates. The thickness of the liquid membrane is approximately 10 μm, about twice the capillary diameter in in vivo peripheral tissues. Irradiation of visible light onto the liquid membrane of HbV coencapsulating FMN and EDTA showed significantly fast rates for the metHb photoreduction. Especially, the coencapsulation of FMN (5 mM) and EDTA (50 mM) completed the metHb photoreduction within only 20 s. This significantly fast photoreduction system would be applicable to the transcutaneous irradiation of visible light to the body for the rejuvenation of HbV when the metHb content increased after the infusion of HbV.

In our study we established an efficient photoreduction system in a nanoparticle as shown in Figure 9. The illuminated visible light excites FMN to convert it to FMN*, and this reacts with an electron donor and transforms to $FMNH_2$, that subsequently reduces ferric metHb to its ferrous form. The reduced Hb can then reversibly bind O_2. Irrespective of the blood substitutes, one advantage of coencapsulation in a nanoparticle is that the concentrations of the components in the vesicles (nanoenvironment) are very high. Accordingly, the desired reactions are significantly accelerated and the

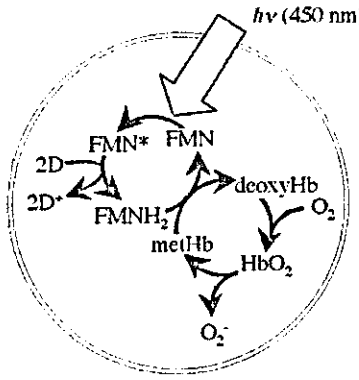

Figure 9. MetHb photoreduction system in a nanoparticle (HbV) using FMN and an electron donor (D), and recovery of the O_2-binding property.

unwanted side reaction is minimized in comparison with the homogeneous solution. To completely eliminate the side reaction of $FMNH_2$ and O_2, photoreduction under anaerobic conditions or coencapsulation of a radical scavenger, such as catalase, would be effective (*29*, *30*). RBC contains NADPH-flavin reductase to reduce metHb (*21*), and the reduced form of flavin is susceptible to react with O_2 as a side reaction. However, our results imply that the highly concentrated condition in RBCs and well-organized radical scavenging system should contribute to the effective metHb reduction in RBCs.

ACKNOWLEDGMENT

Supported by Health Sciences Research Grants (Research on Pharmaceutical and Medical Safety, Artificial Blood Project), the Ministry of Health and Welfare, Japan, 21 COE "Practical Nano-Chemistry" from MEXT, Japan, and Grants in Aid for Scientific Research from the Japan Society for the Promotion of Science (B16300162).

LITERATURE CITED

(1) Tracewell, C. A., Cua, A., Stewart, D. H., Bocian, D. F., and Brudvig, G. W. (2001) Characterization of carotenoid and chlorophyll photooxidation in photosystem II. *Biochemistry 40*, 193−203.

(2) Vorkink, W. P., and Cusanovivh, M. A. (1974) Photoreduction of horse heart cytochrome *c*. *Photochem. Photobiol. 19*, 205−215.

(3) Adar, F., and Yonetani, T. (1978) Resonance Raman spectra of cytochrome oxidase. Evidence for photoreduction by laser photons in resonance with the Soret band. *Biochim. Biophys. Acta 502*, 80−86.

(4) Kitagawa, T., and Nagai, K. (1979) Quaternary structure-induced photoreduction of haem of haemoglobin. *Nature 281*, 503−504.

(5) Kitagawa, T., Chihara, S., Fushitani, K., and Morimoto, H. (1984) Resonance Raman study of subunit assembly dependent photoreduction of heme of extracellular giant hemoglobin. *J. Am. Chem. Soc. 106*, 1860−1862.

(6) Pierre, J., Bazin, M., Debey, P., and Santus, P. (1982) One-electron photoreduction of bacterial cytochrome P-450 by ultraviolet light. *Eur. J. Biochem. 124*, 533−537.

(7) Sakai, H., Onuma, H., Umeyama, M., Takeoka, S., and Tsuchida E. (2000) Photoreduction of methemoglobin by irradiation in the near-ultraviolet region. *Biochemistry 39*, 14595−14602.

(8) McCormick, D. B., Koster, J. F., and Veeger, C. (1967) On the mechanism of photochemical reductions of FAD and FAD-dependent flavoproteins. *Eur. J. Biochem. 2*, 387−391.

(9) Heelis, P. F., Parsons, B. J., Phillips, G. O., and McKellar, J. F. (1979) The photoreduction of flavins by amino acids and EDTA. A continuous and flash photolysis study. *Photochem. Photobiol. 30*, 343−347.

(10) Traber, R., Kramer, H. E. A., and Hemmerich, P. (1982) Mechanism of light-induced reduction of biological redox centers by amino acids. A flash photolysis study of flavin photoreduction by ethylenediaminetetraacetate and nitrilotriacetate. *Biochemistry 21*, 1687−1693.

(11) Massey, V., Strickland, S., Mayhew, S. G., Howell, L. G., Engel, P. C., Matthews, R. G., Schuman, M., and Sullivan, P. A. (1969) The production of superoxide anion radicals in the reaction of reduced flavins and flavoproteins with molecular oxygen. *Biochem. Biophys. Res. Commun.* 36, 891−897.

(12) Massey, V., Stankovich, M., and Hemmerich, P. (1978) Light-mediaated reduction of flavoproteins with flavins as catalyst. *Biochemistry 17*, 1−8.

(13) Cusanovich, M. A., Meyer, T. E., and Tollin, G. (1985) Flavocytochrome *c*: Transient kinetics of photoreduction by flavin analogues. *Biochemistry 24*, 1281−1287.

(14) Sharp, R. E., Moser, C. C., Rabanal, F., and Dutton, P. L. (1998) Design, synthesis, and characterization of a photoactivatable flavocytochrome molecular maquette. *Proc. Natl. Acad. Sci. U.S.A.* 95, 10465−10470.

(15) Hazzard, J. T., Govindaraj, S., Poulos, T. L., and Tollin, G. (1997) Electron transfer between the FMN and heme domains of cytochrome P450 μ_B-3. *J. Biol. Chem. 272*, 7922−7926.

(16) Shumyantseva, V. V., Bulko, T. V., Schmid, R. D., and Archakov, A. I. (2002) Photochemical properties of a riboflavins/cytochrome P450 2B4 comples. *Biosensors Bioelecronics 17*, 233−238.

(17) Shumyantseva, V. V., Bulko, T. V., Schmid, R. D., and Archakov, A. I. (2000) Flavocytochrome P450 2B4 photoreduction. *Biophysics 45*, 982−987 (Translated from *Biofizika*).

(18) Masuda, S., and Bauer, C. E. (2002) AppA is a blue light photoreceptor that antirepresses photosynthesis gene expression in Rhodobacter sphaeroides. *Cell 110*, 613−623.

(19) Tsubota, K., Laing, R. A., and Kenyon, K. R. (1987) Noninvasive measurements of pyridine nucleotide and flavoprotein in the lens. *Invest. Ophthalmol. Vis. Sci. 28*, 785−789.

(20) Brown, W. D., and Synder, H. E. (1969) Nonenzymatic reduction and oxidation of myoglobin and hemoglobin by nicotinamide adenine dinucleotides and flavins. *J. Biol. Chem. 244*, 6702−6706.

(21) Yubisui, T., Takeshita, M., and Yoneyama, Y. (1980a) Reduction of methemoglobin through flavin at the physiological concetration by NADPH-flavin reductase of human erythrocytes. *J. Biochem. 87*, 1715−1720.

(22) Yubisui, T., Matsukawa, S., and Yoneyama, Y. (1980b) Stopped flow studies on the nonenzymatic reduction of methemoglobin by reduced flavin mononucleotide. *J. Biol. Chem. 255*, 11694−11697.

(23) Tsuchida, E. (1998) *Blood Substitutes: present and future perspectives* (Tsuchida, E., Ed.) Elsevier Science, New York.

(24) Takeoka, S., Ohgushi, T., Ohmori, T., Terase, T., and Tsuchida, E. (1996) Layer controlled hemoglobin vesicles by interaction of hemoglobin with phospholipid assembly. *Langmuir 12*, 1775−1779.

(25) Sakai, H., Takeoka, S., Park, S. I., Kose, T., Nishide, H., Izumi, Y., Yoshizu, A., Kobayashi, K., and Tsuchida, E. (1997) Surface modification of hemoglobin vesicles with poly(ethyleneglycol) and effects on aggregation, viscosity, and blood flow during 90% exchange transfusion in anesthetized rats. *Bioconjugate Chem. 8*, 23−30.

(26) Szebeni, J., Hauser, H., Eskelson, C. D., Watson, R. R., and Winterhalter, K. H. (1988) Interaction of hemoglobin derivatives with liposomes. Membrane cholesterol protects against the changes of hemoglobin. *Biochemistry 27*, 6425−6434.

(27) Takeoka, S., Sakai, H., Kose, T., Manò, Y., Seino, Y., Nishide, H., and Tsuchida, E. (1997) Methemoglobin formation in hemoglobin vesicles and reduction by encapsulated thiols. *Bioconjugate Chem. 8*, 539−544.

(28) Sakai, H., Tomiyama, K., Sou, K., Takeoka, S., and Tsuchida, E. (2000) Poly(ethyleneglycol)-conjugation and

deoxygenation enable long-term preservation of hemoglobin vesicles as oxygen carriers. *Bioconjugate Chem. 11*, 425−432

(29) Teramura, Y., Kanazawa, H., Sakai, H., Takeoka, S., and Tsuchida, E. (2003) The prolonged oxygen -carrying ability of Hb vesicles by coencapsulation of catalase in vivo. *Bioconjugate Chem. 14*, 1171−1176.

(30) D'Agnillo, F., and Chang, T. M. (1998) Polyhemoglobin-superoxide dismutase-catalase as a blood substitute with antioxidant properties. *Nat. Biotechnol. 16*, 667−71.

(31) Chang, T. M., Powanda, D., and Yu WP. (2003) Analysis of polyethylene-glycol-polylactide nano-dimension artificial red blood cells in maintaining systemic hemoglobin levels and prevention of methemoglobin formation. *Artif. Cells Blood Substitutes Immobilization Biotechnol. 31*, 231−47.

(32) Everse, J. (1994) Photochemical reduction of methemoglobin and methemoglobin derivatives. *Methods Enzymol. 231*, 524−536.

(33) Sakai, H., Takeoka, S., Yokohama, H., Seino, Y., Nishide, H., and Tsuchida, E. (1993) Purufication of concentrated Hb using organic solvent and heat treatment. *Protein Expression Purif. 4*, 563−569.

(34) Sakai, H., Yuasa, M., Onuma, H., Takeoka, S., and Tsuchida, E. (2000) Synthesis and physicochemical characterization of a series of hemoglobin-based oxygen carriers: objective comparison between cellular and acellular types. *Bioconjugate Chem. 11*, 56−64.

(35) Hatchard, C. G., and Parker, C. A. (1956) A new sensitive chemical actinometer II. Potasium ferrioxalate as a standard chemical actinometer. *Proc. R. Soc. London 235*, 518−536.

(36) Wegner, E. E., and Adamson, A. W. (1966) Photochemistry of complex ions. III. Absolute quantum yields for the photolysis of some aqueous chromium (III) complexes. Chemical actinometry in the long wavelength visible region. *J. Am. Chem. Soc. 88*, 394−404.

(37) Sou, K., Naito, Y., Endo, T., Takeoka, S., and Tsuchida, E. (2003) Effective encapsulation of proteins into size-controlled phospholipid vesicles using freeze−thawing and extrusion. *Biotechnol. Prog. 19*, 1547−1552.

(38) Sou, K., Endo, T., Takeoka, S., and Tsuchida, E. (2000) Poly(ethylene glycol)-modification of the phospholipid vesicles by using the spontaneous incorporation of poly(ethylene glycol)-lipid into the vesicles. *Bioconjugage Chem. 11*, 372−379.

(39) Sakai, H., Tomiyama, K., Masada, Y., Takeoka, S., Horinouchi, H., Kobayashi, K., and Tsuchida, E. (2003) Pretreatment of serum containing Hb-vesicels (oxygen carriers) to avoid interference in clinical laboratory tests. *Clin. Chem. Lab. Med. 41*, 222−231.

(40) Hamachi, I., Nomoto, K., Tanaka, S., Tajiri, Y., and Shinkai, S. (1994) Self-sufficient electron injection from NADH to the active center of flavin-pendant myoglobin. *Chem. Lett. 1994*, 1139−1142.

(41) Matsuo, T., Hayashi, T., and Hisaeda, Y. (2002) Reductive activation of dioxygen by a myoglobin reconstituted with a flavohemin.*J. Am. Chem. Soc. 124*, 11234−11235.

(42) Frati, E., Khatib, A., Front, P., Panasyuk, A., Aprile, F., and Mitrovic, D. R. (1997) Degradation of hyaluronic acid by photosensitized riboflavin in vitro. Modulation of the effect by transition metals, radical quenchers, and metal chelators. *Free Rad. Biol. Med. 22*, 1139−1144.

(43) Sakai, H., Horinouchi, H., Masada, Y., Yamamoto, M., Takeoka, S., Kobayashi, K., Tsuchida, E. (2004) Hemoglobin-vesicles suspended in recombinant human serum albumin for resuscitation from hemorrhagic shock in anesthetized rats. *Crit. Care Med. 32*, 539−545.

BC049913Z

0022-3565/05/3122-702–709$20.00
THE JOURNAL OF PHARMACOLOGY AND EXPERIMENTAL THERAPEUTICS
Copyright © 2005 by The American Society for Pharmacology and Experimental Therapeutics
JPET 312:702–709, 2005

Vol. 312, No. 2
74534/1187652
Printed in U.S.A.

Circulation Kinetics and Organ Distribution of Hb-Vesicles Developed as a Red Blood Cell Substitute

Keitaro Sou, Robert Klipper, Beth Goins, Eishun Tsuchida, and William T. Phillips

Advanced Research Institute for Science and Engineering, Waseda University, Tokyo, Japan (K.S., E.T.); and Department of Radiology, University of Texas Health Science Center at San Antonio, San Antonio, Texas (R.K., B.G., W.T.P.)

Received July 20, 2004; accepted September 30, 2004

ABSTRACT

Phospholipid vesicles encapsulating concentrated human hemoglobin (Hb-vesicles, HbV), also known as liposomes, have a membrane structure similar to that of red blood cells (RBCs). These vesicles circulate in the bloodstream as an oxygen carrier, and their circulatory half-life times ($t_{1/2}$) and biodistribution are fundamental characteristics required for representation of their efficacy and safety as a RBC substitute. Herein, we report the pharmacokinetics of HbV and empty vesicles (EV) that do not contain Hb, in rats and rabbits to evaluate the potential of HbV as a RBC substitute. The samples were labeled with technetium-99m and then intravenously infused into animals at 14 ml/kg to measure the kinetics of HbV elimination from blood and distribution to the organs. The $t_{1/2}$ values were 34.8 and 62.6 h for HbV and 29.3 and 57.3 h for EV in rats and rabbits, respectively. At 48 h after infusion, the liver, bone marrow, and spleen of both rats and rabbits had significant concentrations of HbV and EV, and the percentages of the infused dose in these three organs were closely correlated to the circulatory half-life times in elimination phase ($t_{1/2\beta}$). Furthermore, the milligrams of HbV per gram of tissue correlated well between rats and rabbits, suggesting that the balance between organ weight and body weight is a fundamental factor determining the pharmacokinetics of HbV. This factor could be used to estimate the biodistribution and the circulation time of HbV in humans, which is estimated to be equal to that in rabbit.

Hemoglobin (Hb) isolated and purified from red blood cells (RBCs) has been tested as a principal component of RBC substitutes for carrying oxygen. However, the plasma retention time of isolated Hb is particularly short (half-life of ~0.5–1.5 h) because of the dissociation of the Hb tetramer into the dimeric form, which is subsequently filtered by the kidney, and it is known that this dimeric form is nephrotoxic (Savitsky et al., 1978). The potential of phospholipid vesicles as effective carriers of proteins and other bioactive materials has previously been proposed, since the cellular structure of such vesicles can protect the entrapped material from degradation and improve the biodistribution of proteins and other bioactive materials (Gregoriadis and Neerunjun, 1974; Papahadjopoulos et al., 1991). Phospholipid vesicles encapsulating concentrated Hb (HbV) have been proposed as a promising candidate RBC substitute, because encapsulation of Hb within a lipid membrane decreases potential side effects and toxicity of Hb, thereby making vesicles more RBC-like (Djordjevich and Miller, 1980; Gaber and Farmer, 1984; Tsuchida, 1998). The study of the safety and efficacy of HbV formulations by our research group has led to the development of an HbV formulation as a promising candidate for introduction into clinical trials (Tsuchida, 1998; Sakai et al., 2000b, 2001, 2004b; Takeoka et al., 2002).

Determination of the circulation time (half-life) of vesicles has been an important research focus, especially in RBC substitute development, because prolonged oxygen delivery is a required property for an artificial oxygen carrier. There are many reports describing the pharmacokinetics of vesicles, especially in mice and rats; however, it is difficult to apply these published data to the quantitative simulation of a clinical application. This is because of the lack of understanding of the species dependence of relevant mechanisms and correlative factors related to the clearance kinetics of vesicles. Some reports suggest that the circulatory half-life of vesicles injected in small doses into small animals such as

This work was supported in part by project of Health Science Research Grants (Artificial Blood Project) from the Ministry of Health, Labor and Welfare, Japan. K.S. was an overseas Research fellow of the Society of Japanese Pharmacopoeia (2002).

Article, publication date, and citation information can be found at http://jpet.aspetjournals.org.

doi:10.1124/jpet.104.074534.

ABBREVIATIONS: RBC, red blood cell; HbV, hemoglobin vesicle(s); EV, empty vesicle(s); ^{99m}Tc, technetium-99m; PEG, polyethylene glycol; DPPC, 1,2-dipalmitoyl-*sn*-glycero-3-phosphocholine; DPEA, 1,5-dihexadecyl-L-glutamate-*N*-succinic acid; PEG-DSPE, 1,2-distearoyl-*sn*-glycero-3-phosphoethanolamine-*N*-[monomethoxy poly(ethylene glycol) (5000)]; PLP, pyridoxal-5′ phosphate; HMPAO, hexamethylpropyleneamine oxime; %ID, percentage of infused dose; MPS, mononuclear phagocyte system.

mice or rats empirically corresponds to half-lives that are 2 or 3 times longer in humans (Gabizon et al., 2003). In addition, the infusion dose of HbV as a RBC substitute, in terms of lipid content, is nearly a hundred times larger compared with other therapeutic uses of vesicles, even though HbV encapsulate a highly concentrated form of Hb (35–40 g/dl). Furthermore, there are many other factors such as the lipid formulation (Allen et al., 1989), vesicle size (Awasthi et al., 2003), and surface modification (Klibanov et al., 1990) that influence the circulation time and distribution of the infused vesicles. There are no clinical data available for using large infusion doses of vesicles such as those required for a RBC substitute. Therefore, we focused this research on determining the correlation factors between data from different species to simulate the pharmacokinetics of HbV. In addition, empty vesicles (EV) that do not contain Hb were studied as a reference to clarify the specific influence of encapsulated Hb on the circulation properties of the vesicles.

Scintigraphic imaging is a particularly powerful tool that can be used to develop and evaluate the formulation of vesicles (Goins and Phillips 2001). Using imaging, Phillips et al. have reported on the pharmacokinetics of liposome-encapsulated Hb radiolabeled with technetium-99m (^{99m}Tc) (Rudolph et al., 1991; Phillips et al., 1992, 1999) and achieved a formulation with long circulation times. These liposomes had a small size (<200 nm), neutral surface, and PEG modification (10 mol%), and were regarded as long-circulating vesicles (so-called stealth liposomes) ($t_{1/2}$ was 65 h after 25% intravenous top-load in rabbits) (Phillips et al., 1999). However, this particular liposome formulation had a low efficiency of Hb encapsulation, because the requisites for stealth liposomes, such as small size, neutral surface, and dense PEG modification were a disadvantage for efficient Hb encapsulation (Perkins et al., 1993; Nicholas et al., 2000). As mentioned above, the infused dose of RBC substitutes will be extremely high, so high encapsulation efficiency of Hb is essential for a successful oxygen-carrying RBC substitute. We have developed HbV with a lipid formulation and encapsulation conditions that have improved the encapsulation efficiency (Takeoka et al., 1996; Sou et al., 2003), and the present HbV formulation has an oxygen-carrying capacity equal to RBCs because of this higher encapsulation efficiency (1.7–2.0 g of Hb per gram of lipids). This article is the first report on the detailed pharmacokinetics of this HbV formulation using scintigraphic imaging of ^{99m}Tc-HbV for monitoring the circulation properties and biodistribution. Factors that would permit estimation of human pharmacokinetics of large quantities of vesicles are discussed.

Materials and Methods

Materials. 1,2-Dipalmitoyl-*sn*-glycero-3-phosphocholine (DPPC), cholesterol, and 1,5-dihexadecyl-L-glutamate-*N*-succinic acid (DPEA) were purchased from Nippon Fine Chemical Co., Ltd. (Osaka, Japan); 1,2-distearoyl-*sn*-glycero-3-phosphoethanolamine-*N*-[monomethoxy poly(ethylene glycol) (5000)] (PEG-DSPE) was purchased from NOF Co. (Tokyo, Japan). DPPC, cholesterol, DPEA, and PEG-DSPE were dissolved in alcohol at a molar ratio of 5, 5, 1, and 0.033, respectively, atomized, and evaporated using a spray dryer (Cracks) to prepare a lipid powder, at Nippon Fine Chemical Co., Ltd. The mixed lipid powder was hydrated with NaOH solution, submitted to three cycles of freeze-thawing, and the resultant dispersion was then lyophilized at Kanto Chemical Co. (Tokyo, Japan). The Hb solution was obtained from outdated donated blood (Japanese Red Cross) according to the purification method described previously (Sakai et al., 2002). The Hb solution (oxyhemoglobin) was converted to carbonylHb by purging the solution with 100% carbon monoxide until testing proved conversion (99% < HbCO). The final concentration of Hb was adjusted to 40 g/dl. Homocysteine, pyridoxal-5′ phosphate (PLP), and glutathione were purchased from Sigma-Aldrich (St. Louis, MO).

Preparation of HbV. HbV were prepared according to a method described previously (Takeoka et al., 1996; Tsuchida, 1998; Sakai et al., 2001; Sou et al., 2003). All HbV preparation work was performed under sterile conditions. The purified carbonylHb solution (40 g/dl) containing 5 mM homocysteine and pyridoxal-5′ phosphate [PLP/Hb ratio of 2.5 (mol/mol)] was mixed with the lyophilized powder containing the mixed lipids (DPPC, cholesterol, DPEA, and PEG-DSPE). After controlling the size of the HbV with an extrusion method (final pore size of the filter, 0.22 μm, Fuji microfilter; Fuji Photo Film Co., Tokyo, Japan), the unencapsulated Hb was removed by three ultracentrifugation steps ($10^5 g$, 30 min each). CarbonylHb was converted to OxyHb by exposure to visible light in an atmosphere of O_2. HbV were suspended in a physiological salt solution and filtered through sterilized filters (pore size, 0.45-μm Dismic; Toyo Roshi, Tokyo, Japan) and deoxygenated by bubbling with N_2 before storage (Sakai et al., 2000a). The control EV encapsulating glutathione (30 mM) was prepared using the same extrusion method.

Characterization of HbV and EV. The characteristics of HbV and EV are summarized in Table 1. The concentrations of Hb and phospholipid were determined by a cyanomethemoglobin method (Hemoglobin Test Wako; Wako Pure Chemicals, Tokyo, Japan) and the cholineoxidase method (Phospholipid C Test Wako; Wako Pure Chemicals), respectively. The encapsulation efficiency of Hb was represented as a w/w ratio of [Hb]/[lipid]. Methemoglobin and carbonylHb content were determined by spectrophotometry (Van Assendelft, 1970). The diameters of the resulting HbV (247 ± 44 nm) and EV (259 ± 32 nm) were determined using a submicron particle analyzer (N4SD; Beckman Coulter, Fullerton, CA). Endotoxin contamination was determined to be below 0.2 EU/ml by the *Limulus* assay test (Sakai et al., 2004a).

^{99m}Tc-Labeling of HbV and EV. Radiolabeling of HbV was performed according to a method described previously (Phillips et al., 1992). A saline solution of sodium [^{99m}Tc]pertechnetate (5 ml, 75 mCi) (Nycomed Amersham, San Antonio, TX) was injected into a vial containing lyophilized hexamethylpropyleneamine oxime (HMPAO, 0.5 mg, $SnCl_2$, 7.6 μg) (Ceretec; Amersham Biosciences Inc., Piscataway, NJ). The mixed solution was incubated for 5 min at room temperature. The ^{99m}Tc-HMPAO solution (1 ml) was then added to the HbV suspension ([Hb]; 10 g/dl, 1 ml), and the resulting mixed solution was incubated for 1 h. After removing free ^{99m}Tc-HMPAO by gel filtration (Sephadex-G25 column), total radioactivity was measured in a dose calibrator (Mark 5 model; Radex, Houston, TX) and the labeling efficiency (E) was calculated as the percentage of post-radioactivity in ^{99m}Tc-HbV to preradioactivity. The ^{99m}Tc-HbV suspension was mixed with unlabeled HbV suspension and the resultant HbV suspension ([Hb], 9.5 g/dl; [lipid], 4.75 g/dl) was used for the experiment. The ^{99m}Tc-EV were also prepared with same method and the lipid concentration was adjusted to the same lipid concentration as that of HbV suspension tested ([lipid], 4.75 g/dl). The ^{99m}Tc-labeled HbV and EV dispersion (0.5 ml) was mixed with rat

TABLE 1
Characteristics of ^{99m}Tc-HbV and ^{99m}Tc-EV suspensions

Parameter	^{99m}Tc-HbV	^{99m}Tc-EV
[Hb][a] (g/dl)	9.5	0
[Lipids] (g/dl)	4.75	4.75
Particle diameter (nm)	247 ± 44	259 ± 32
Endotoxin level (EU/ml)	< 0.2	< 0.2

[a] Methemoglobin, <1%; carbonylHb, <2%.

plasma (1.5 ml) from a donor rat and incubated at 37°C to check the labeling stability. A 100-μl aliquot of incubated sample at 48 h after mixing was passed through a Bio Gel A-15m (200–400 mesh) spin column. The sample was eluted by sequential addition of 100 μl of Dulbecco's phosphate-buffered saline (pH 7.3) under the centrifugal force of 1000 rpm for 1 min. Each fraction was collected separately and counted in a scintillation well counter (Canberra multichannel analyzer; Canberra Industries, Meriden, CT). Another 100-μl aliquot of incubation sample was used as a standard. The sum total of activity eluted with HbV or EV fractions was compared with total radioactivity in the standard.

Animal Experiments. Animal experiments were performed under the National Institutes of Health Animal Use and Care guidelines and approved by the University of Texas Health Science Center at San Antonio Institutional Animal Care Committee. Male Sprague-Dawley rats (200–274 g) were anesthetized with 3% isoflurane (VedCo, St. Joseph, MO) in 100% oxygen gas. Rats were then placed in the supine position under a Picker (Cleveland, OH) large-field-of-view gamma camera using a low-energy, all-purpose collimator and interfaced with a Pinnacle imaging computer (Medasys, Ann Arbor, MI). Image acquisition was begun as HbV or EV were infused into the tail vein at 1 ml/min. Each rat received a total dose of 0.17 to 0.37 mCi of ^{99m}Tc activity, Hb: 1.33 g/kg b.wt.; lipids: 0.67 g/kg b.wt. as an equivalent of 14 ml/kg for the HbV group (n = 5) and 0.48 to 0.55 mCi of ^{99m}Tc activity, lipids: 0.67 g/kg as 14 ml/kg for the EV group (n = 5). The infused dose (in volume) was estimated to be 25% of blood volume where the total blood volume was assumed to be 5.6% of body weight (Frank, 1976). The rabbit experiment was performed in the same manner. Male New Zealand White rabbits (2.2–2.9 kg) were anesthetized with an intramuscular injection of ketamine/xylazine (both from Phoenix Scientific, St. Joseph, MO) mixture (50 and 10 mg/kg body weight, respectively). One ear of a rabbit was catheterized with a venous line, and the other ear was catheterized with an arterial line. HbV or EV was infused in the venous line at 1 ml/min under the same gamma camera, and the blood samples were drawn from the arterial line. Each rabbit received a total dose of 3.7 to 4.5 mCi of ^{99m}Tc activity, Hb: 1.36 g/kg b.wt.; lipids: 0.68 g/kg b.wt. as 14.25 ml/kg for the HbV group (n = 5) and 3.5 to 4.9 mCi, lipids: 0.68 g/kg as 14.25 ml/kg for the EV group (n = 4). The infused dose (in volume) was estimated to be 25% of blood volume where the total blood volume was assumed to be 5.7% of body weight (Kozma et al., 1974).

Image Analysis. One-minute dynamic 64 × 64 pixel scintigraphic images were acquired over a continuous period of 0.5 and 2 h for rats and rabbits after the infusion of HbV or EV, respectively. Static images were also acquired at 3, 6, 12, 24, 36, and 48 h postinfusion. The image analysis was performed using a nuclear medicine analysis workstation (Pinnacle computer; Medasys). The regions of interest were drawn over the whole body, liver, and spleen in images. The counts of radioactivity were decay-corrected at each time and converted to a percentage of the whole body counts. Corrections were made for the blood pool contribution of the liver and spleen of the rat (17 and 6%, respectively, of the total blood volume). For rabbit, the liver was corrected by 25.4% of the total blood volume, and the spleen was individually corrected by 1.047 ± 0.076% for HbV and 1.592 ± 0.049% of the total blood volume for EV as percentage of infused dose (%ID) just after infusion, respectively.

Blood Persistence and Biodistribution. Blood was collected from the tail vein of the rat or arterial line of the rabbit (50 or 100 μl) at various times postinfusion. The radioactivity of blood samples was quantified in a scintillation well counter (Canberra multichannel analyzer; Canberra Industries) at the same time. The counts at each time were converted to the percentage of the counts of sample collected immediately after infusion. The elimination rate constants (k) were calculated by the least-squares method and half-life time ($t_{1/2}$) was calculated from eq. 1.

$$t_{1/2} = \frac{0.693}{k} \quad (1)$$

The animals were rapidly sacrificed at 48 h, and the tissue samples were collected, weighed, and counted for radioactivity in a scintillation well counter (Canberra multichannel analyzer; Canberra Industries) to calculate the biodistribution. To calculate the %ID per organ, total blood volume, muscle, and skin mass were estimated as 5.6, 40, and 13% of total body weight for rat (Frank, 1976; Petty, 1982), and 5.7, 45, and 10% of total body weight for rabbit (Kozma et al., 1974; Kaplan and Timmons, 1979), respectively. The bone was estimated as 10% of total body weight for rat (Frank, 1976; Petty, 1982) and 12 times the femur weight for rabbit (Dietz, 1944).

Estimation of the Biodistribution in Humans. The total Hb or lipids per organ (Ws) was calculated from the %ID and ID of Hb or lipids in terms of weight.

$$Ws(\text{mg}) = \frac{\%\text{ID} \times \text{ID}}{100} \quad (2)$$

The organ weight (Wo) of experimental animals was measured by an electronic balance and the Hb per organ weight (R) was calculated.

$$R(\text{mg/g}) = \frac{Ws}{Wo} \quad (3)$$

Ws was calculated from eq. 3 for humans, where the weights of liver, spleen, and bone (Wo) were estimated as 1.8, 0.18, and 5.0 kg, respectively, for average humans (70 kg) (International Commission on Radiological Protection, 1984), and the R value was applied as an average value between rats and rabbits shown in Table 4 for each organ. The ID of HbV ([Hb] = 9.5 g/dl, [lipids] = 4.75 g/dl) was calculated to be 25% of the blood volume (4.9 liters, 70 ml/kg b.wt.), and the %ID was calculated from eq. 2. The half-life times ($t_{1/2\beta}$) were estimated from eq. 4, where, constant value (C) was determined as a slope of the fitting line in this study and $\%\text{ID}_{\text{total}}$ was sum values of %ID for liver, spleen, and bone.

$$t_{1/2\beta} = \frac{C}{\%\text{ID}_{\text{total}}} \quad (4)$$

Statistical Methods. Values are reported as mean ± S.E.M. Statistical analysis was performed using Microsoft Excel for Windows. The image analysis and biodistribution data were compared using the Student's unpaired t test. A P value <0.01 or 0.05 was considered statistically significant.

Results

Labeling Efficiencies. The labeling efficiencies of ^{99m}Tc-HbV and ^{99m}Tc-EV were 69.1 ± 2.0% (n = 2) and 75.6 ± 5.1% (n = 3) for the rat studies, and 62.0 ± 4.8% (n = 5) and 70.9 ± 2.1% (n = 2) for the rabbit studies. Labeling efficiencies were similar for both ^{99m}Tc-HbV and ^{99m}Tc-EV, even though ^{99m}Tc-HbV used homocysteine and ^{99m}Tc-EV used glutathione. The ^{99m}Tc would be located in the inner aqueous phase of vesicles, and both homocysteine and Hb of HbV, and glutathione of EV would possibly bind the ^{99m}Tc (Rudolph et al., 1991; Phillips et al., 1992). The incubation of labeled HbV and EV in serum for 48 h revealed that 5 and 4% of the ^{99m}Tc dissociated from HbV and EV, indicating that the labeling was very stable and the contents were stably encapsulated inside the vesicles.

Circulation Kinetics. To determine the circulation kinetics as shown in Fig. 1, a and b, the radioactive counts of blood samples were plotted as a percentage of the counts for blood sample collected immediately at the end of the infusion with

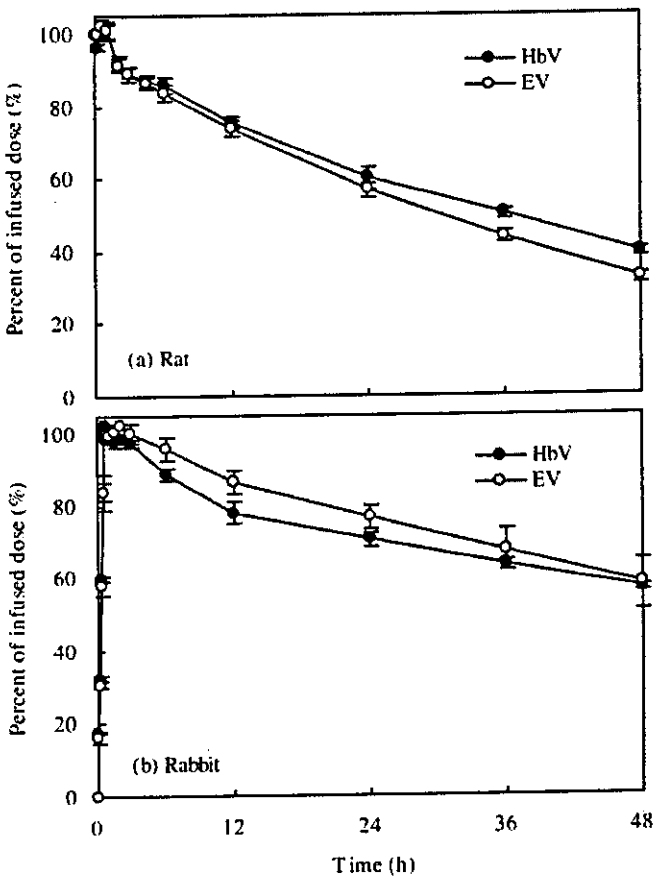

Fig. 1. Circulation kinetics of HbV and EV after top-loading intravenous infusion (14 ml/kg) in rats and rabbits. The radioactivity was determined by scintillation counting of blood samples with time. The percentage of radioactivity is calculated as a percentage of baseline radioactivity in a blood sample withdrawn just after HbV or EV infusion.

time. The elimination profiles of infused HbV showed two components with an initial fast clearance followed by a slower clearance phase, which is regarded as a distribution (α) phase in the mononuclear phagocyte system (MPS) and an elimination (β) phase, respectively. The clearance rate constant in the distribution phase of HbV was equal to that of EV, and k_β was 1.3 times smaller than that of EV in rats as shown in Table 2. The circulation half-life times ($t_{1/2}$ values) associated with both the distribution and elimination phases of HbV and EV in rats were 34.8 and 29.3 h, respectively. The clearance rates of HbV and EV were slower in rabbits compared with those in rats, especially for the distribution phase. The k_α of HbV was 0.0226 h^{-1} in rabbit, which was one-quarter of that in rats and 1.4 times larger than that of EV in rabbit. k_β for HbV was 1.3 times smaller than that of EV. The $t_{1/2}$ values of HbV and EV were 62.6 and 57.3 h in rabbits, respectively.

Imaging Study. The gamma camera images of rats or rabbits receiving HbV were acquired at various times to determine the organ distribution profiles with time. As shown in Figs. 2 and 3, radioactivity was observed over the whole body of animals and in the heart, demonstrating that HbV were circulating. Immediately after infusion, the heart, liver, and spleen were identified because these organs had a large blood pool volume, and the relative intensities of the liver and spleen increased in comparison with the heart with time. The %ID in liver and spleen calculated from gamma camera images with decay correction and correction for blood pool contribution are shown in Fig. 4. The %ID in liver was increased during the infusion and decreased after the infusion ended, especially in HbV as shown in Fig. 4, a and c. This initial decrease was most likely due to the adjustment of blood volume after top-loading. The values of %ID in liver and spleen were quickly increased during the first 6 to 12 h after infusion and reached a plateau at 48 h. At 48 h, the liver had 10.9 ± 0.8 and 7.6 ± 1.0% of HbV in rats and rabbits, respectively, whereas the spleen had 6.6 ± 0.3 and 0.98 ± 0.14% of HbV in rats and rabbits, respectively.

Biodistribution. The detailed biodistribution data of HbV at 48 h are shown in Table 3. HbV could be precipitated easily by ultracentrifugation of blood sample, and no Hb was detected in the supernatant serum in the blood sample for 48 h. In addition, no Hb was detected in urine for 48 h supporting that the Hb was not eluted from vesicles during circulation. HbV and EV were mainly distributed in liver, bone marrow, and spleen, and the %ID values for HbV were smaller than those of EV in these organs. Relatively high values for the bowel, feces, and urine were likely due to metabolism during excretion of HbV. The sum values of %ID for liver, spleen, and bone ($\%ID_{total}$), which are the main organs for MPS uptake, were 26.60 and 13.64% for HbV and 36.36 and 17.84% for EV in rats and rabbit, respectively. The corresponding $t_{1/2\beta}$ values given in Table 2 were 39.1, 79.2, 30.1, and 60.2 h, respectively. These $t_{1/2\beta}$ values are in proportion to the reciprocal of $\%ID_{total}$ as shown in Fig. 5, and the constant value (C) in eq. 4 was determined to be 1074.1 as a slope of the fitting line.

The calculated total lipids and Hb doses (in milligrams) delivered to the liver, bone, and spleen are summarized in Table 4. These values are independent of the species dependence of relative weight balances of organs in whole body and represent the amount of uptake of the HbV in a gram of each organ. The spleen had 14.43 ± 0.54 and 14.92 ± 1.25 mg of Hb per gram in rat and rabbit, and the liver and bone also had similar values in rat and rabbit.

Discussion

The improvement in oxygen-carrying capacity of HbV as a RBC substitute requires longer circulation and a higher en-

TABLE 2
Kinetic parameters of HbV and EV clearance from blood in rats and rabbits (25% top-loading)

Animal	Sample	Distribution (α) Phase		Elimination (β) Phase		$t_{1/2}$
		k_α	$t_{1/2\alpha}$	k_β	$t_{1/2\beta}$	
		h^{-1}	h	h^{-1}	h	
Rat	HbV	0.0894	7.8	0.0177	39.1	34.8
	EV	0.1004	6.9	0.0230	30.1	29.3
Rabbit	HbV	0.0226	30.7	0.0088	79.2	62.6
	EV	0.0159	43.6	0.0115	60.2	57.3

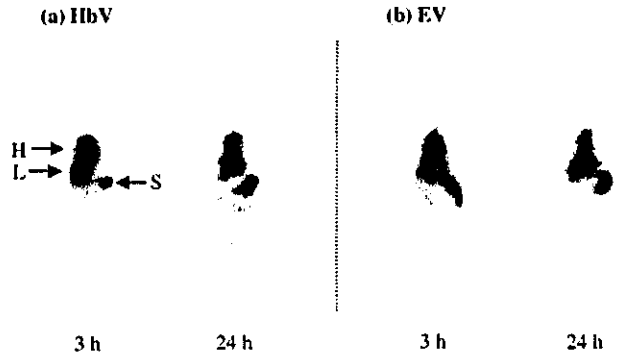

Fig. 2. Static gamma camera images of whole body of rats infused with HbV or EV acquired at 3 and 24 h after infusion. The images were acquired for 1 min at 3 h and 2 min at 24 h. The arrows show heart (H), liver (L), and spleen (S).

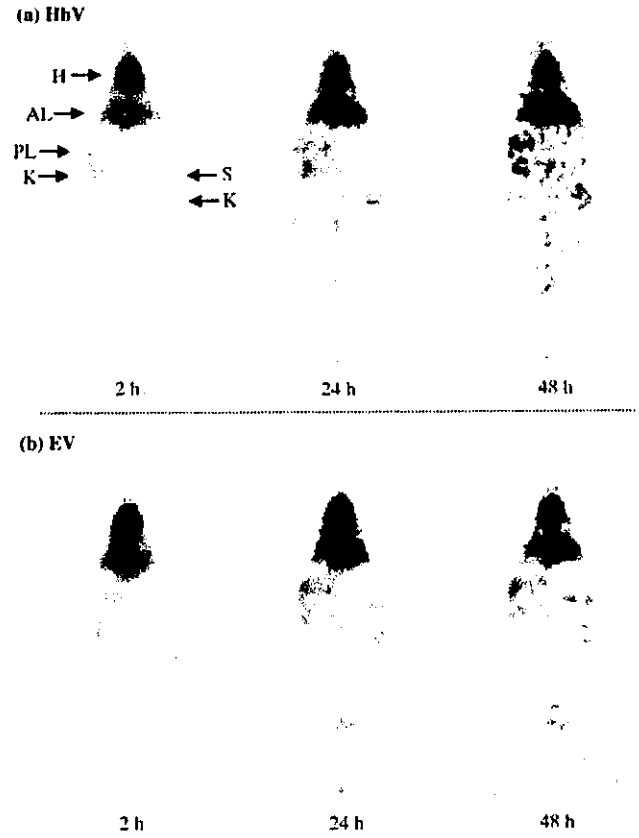

Fig. 3. Static gamma camera images of rabbits acquired at 2, 24, and 48 h after HbV or EV infusion. The images were acquired for 1 min at 2 h, 2 min at 24 h, and 5 min at 48 h. The arrows indicate heart (H), anterior liver (AL), posterior liver (PL), spleen (S), and kidney (K).

capsulation efficiency of Hb. The HbV formulation described in this study has high encapsulation efficiency ([Hb]/[lipid] = 2.0), and a circulatory half-life time of 34.8 and 62.6 h in rats and rabbits, respectively. This value is equal to the 65-h circulation half-life time for a PEG-liposome-encapsulated Hb formulation with a long circulation time in rabbits (Phillips et al., 1999). Other long-circulation vesicle formulations are successful for therapeutic uses such as cancer therapy or antibacterial treatment (Papahadjopoulos et al., 1991; Gabizon et al., 2003). However, the characteristics of small size (below 200 nm), neutral surface, and incorporation of significant amounts of PEG-lipid (5–10 mol%) of these formulations are ineffective in encapsulating Hb into vesicles (Perkins et al., 1993; Nicholas et al., 2000). The HbV formulation described in the present study is mainly composed of DPPC and cholesterol, only 0.3 mol% of PEG-lipid to prevent aggregation of the vesicles (Sakai et al., 2000a; Sou et al., 2000), and 9 mol% of anionic DPEA to reduce the lamellarity of the bilayer membrane (Sou et al., 2003). In general, anionic phospholipids such as phosphatidylglycerol or phosphatidylserine are used for the preparation of anionic vesicles; however, some side effects such as complement and platelet activations have been reported (Reinish et al., 1988). These immunological responses accelerate plasma protein adsorption on the surface of vesicles (opsonins) and then those vesicles are rapidly trapped into MPS. Our DPEA has a carboxylic group to negatively charge the surface of vesicles instead of a phosphate group of anionic phospholipids, and it does not have side effects like those reported for phosphatidylglycerol-containing vesicles (Wakamoto et al., 2001). The safety studies of HbV are underway, and the initial results in rats suggest that the DPEA vesicles have fewer side effects on immunological responses such as complement activation and thrombocytopenia compared with vesicles containing other anionic phospholipids. This bioinactive surface imparted by DPEA contributes to the stable circulation of HbV.

The diameter of vesicles is also an important factor for circulation kinetics and encapsulation efficiency. Recently, Awasthi et al. (2003) reported that the maximum size to show long circulation characteristics of PEG vesicle was around 240 nm in rabbits. The larger size of HbV is advantageous for the encapsulation efficiency of Hb; however, 250-nm HbV is of maximum and reasonable size to satisfy both long circulation and high Hb content requirements. We satisfied both long-circulation and high encapsulation efficiency of Hb by developing the lipid formulation and strictly regulating the diameter by the extrusion method. The clear effect of encapsulated Hb on the circulation time of vesicles was prolongation of the β phase for both animals. This is most likely due to greater saturation of the MPS by the encapsulated Hb.

Biodistribution data showed that HbV and EV were mainly distributed into liver, spleen, and bone. We have already clarified that Hb and phospholipid from HbV readily disappeared from the Kupffer cells in liver and macrophages in spleen in rats within a week after administration (Sakai et al., 2001). The trapping of HbV in MPS is regarded as a normal physiological pathway for removal of aged RBC; therefore, this should be a reasonable pathway for the elimination and metabolism of Hb-based RBC substitutes. The importance of the biodistribution of Hb-based RBC substitutes has been discussed and a vasoconstrictive effect of modified Hbs has been indicated (Sakai et al., 2000b). These side effects are triggered by the unusual biodistribution of small-sized modified Hb (<100 nm) to smooth muscle across the endothelium or the space of Disse in fenestrated endothelium of hepatic sinusoids, where the vasorelaxation factors nitric oxide and carbon monoxide are bound to Hb (Goda et al., 1998). The smaller vesicles might be effective for longer circulation of encapsulated Hb, but this would have the risk of causing similar or unusual side effects as those observed for modified Hb.

As summarized in Table 3, the %ID of HbV and EV in biodistribution data at 48 h is significantly different between

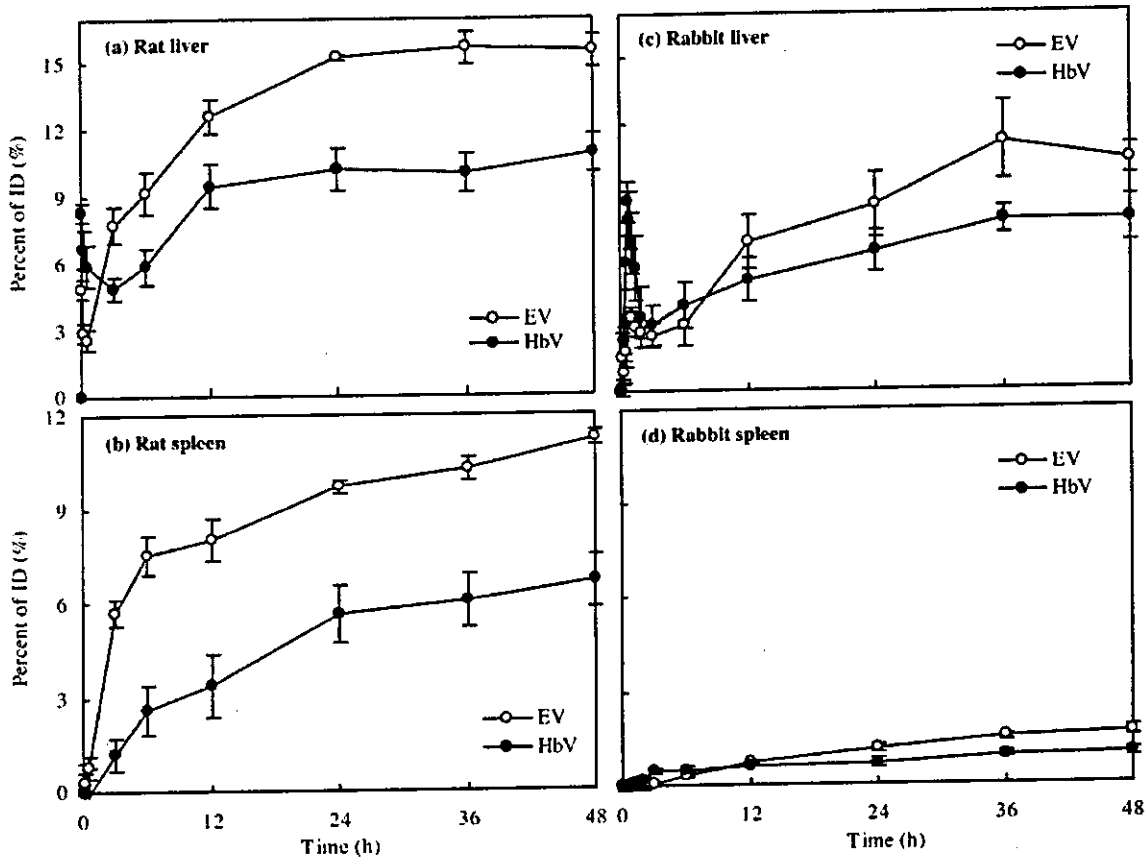

Fig. 4. %ID for liver and spleen calculated from the gamma camera image acquired at particular times and after decay correction. The blood pool contribution was corrected using values of 17 and 6% of the total blood volume for liver and spleen in rats, respectively. For rabbit, the liver was corrected by 25.4% of the total blood volume, and the spleen was individually corrected by 1.047 ± 0.076% for HbV and 1.592 ± 0.049% of the total blood volume for EV as %ID of just after infusion, respectively.

rats and rabbits ($P < 0.05$ for many organs). The rat had more HbV and EV in liver, bone, and especially spleen and less HbV and EV in blood. These data suggest that the biodistribution pattern of vesicles was not specifically changed by the encapsulation of Hb or the animal species tested; however, the quantitative values of %ID were significantly affected by these factors. Image analysis showed that the %ID required for saturating the liver and spleen with time was as shown in Fig. 4. The former liposome encapsulated Hb, which had non-PEG, showed significantly greater %ID (liver, 15.4 ± 2.1% ID; spleen, 18.1 ± 3.3% ID) in rabbit (Rudolph et al., 1991). The "saturated" level observed at those infusion doses would be determined by the balance between rate of uptake from the circulation, which was strongly affected by the HbV formulation and the rate of metabolic processing. The full saturation of MPS by the increased infusion dose of HbV might diminish the difference of pharmacokinetics between HbV formulations because the metabolic processing should become dominant factor. At 48 h, the blood clearance was in the slower β phase (Fig. 1) so that the inverse proportion between %ID and $t_{1/2\beta}$ is reasonable, and the determined constant C is available to estimate the $t_{1/2\beta}$ from the %ID. In addition, we have discovered that the most important factor for explaining the difference of %ID accumulating in the organs of the MPS between species is due to the different ratio of organ weight to body weight between species. For example, the average spleen weights of the experimental animals for HbV were 0.65 ± 0.07g in rats (216 ± 20 g b.wt., $n = 5$) and 0.87 ± 0.21 g in rabbits (2670 ± 97 g b.wt., $n = 5$). Therefore, the ratio of organ weight to body weight of rats is 9 times larger than that of rabbits, which means that rats have a 9 times larger mass capacity in spleen at the same infusion dose based on body weight. When the uptake of HbV is calculated in terms of mg of lipid and Hb per gram of MPS organ, the values in rats and rabbits are very close to each other as summarized in Table 4, indicating that the concentration of HbV in these organs was species-independent in this case. These values can be used to quantitatively estimate biodistribution of HbV based on organ weight. By using these two factors of C values and milligrams of lipids per organ weight, we were able to roughly estimate the biodistribution and circulation time of HbV in humans (see *Materials and Methods*). Laverman et al. (2000) reported that the distribution pattern of PEG-liposomes in humans was similar to that of rats and rabbits, with high uptake in liver, spleen, and bone marrow. Other biodistribution studies of vesicles also suggested a high uptake in liver, spleen, and bone marrow in humans (Dams et al., 2000; Gabizon et al., 2003), and these reports support our estimation. Based on the MPS organ weights of average humans and the milligrams of uptake of lipid and hemoglobin per gram MPS organs at 48 h (human liver weight, 1.8 kg; human spleen, 0.18 kg; and human bone, 5.0 kg) (International Commission on Radiological Protection, 1984), we estimated that %IDs of HbV are 5.4% (liver), 4.5% (spleen), and 6.4% (bone), and a $t_{1/2\beta}$ of approximately 66 h in humans after a 25% top-loading